Mechanics of In-situ Leaching

Attempt at Understanding
Using Experiments and Models

Herbert Einstein

Mechanics of In-situ Leaching

Background

In-situ leaching and tailings

In situ leaching is being used

Bulk: Rock Salt, Potash

From internal surfaces: Uranium, Copper, Gold

In situ leaching

Can reduce but not eliminate tailings

Leaching is often used in tailings deposits

Mechanics of In-situ Leaching
Introduction

In-situ leaching on internal surfaces in the ground

Needs an opening in the ground:
- Natural Opening such as pores or fractures
- Artificially created opening (widening an existing one or crating a new one

Need medium going through opening

Needs medium to remove/transport minerals

To understand the mechanics of all this we will show with experiments and models:

How one represents fracture networks and flow through fracture networks	DISCRETE FRACTURE NETWORK GEOFRAC & GEOFRAC FLOW/THERMAL FRACTURE FLOW AND TRANSPORT
How one creates new fractures or extends existing ones through	HYDRAULIC FRACTURING
How one creates other openings or extends existing ones through	DISSOLUTION

Mechanics of In-situ Leaching

Background and Introduction

Discrete Fracture Network -
GEOFRAC/GEOFRAC FLOW/GEOFRAC THERMAL

Fracture Flow and Transport

Hydraulic Fracturing

Dissolution

Conclusions

Fracture Systems - Geometry

Fracture Systems Flow

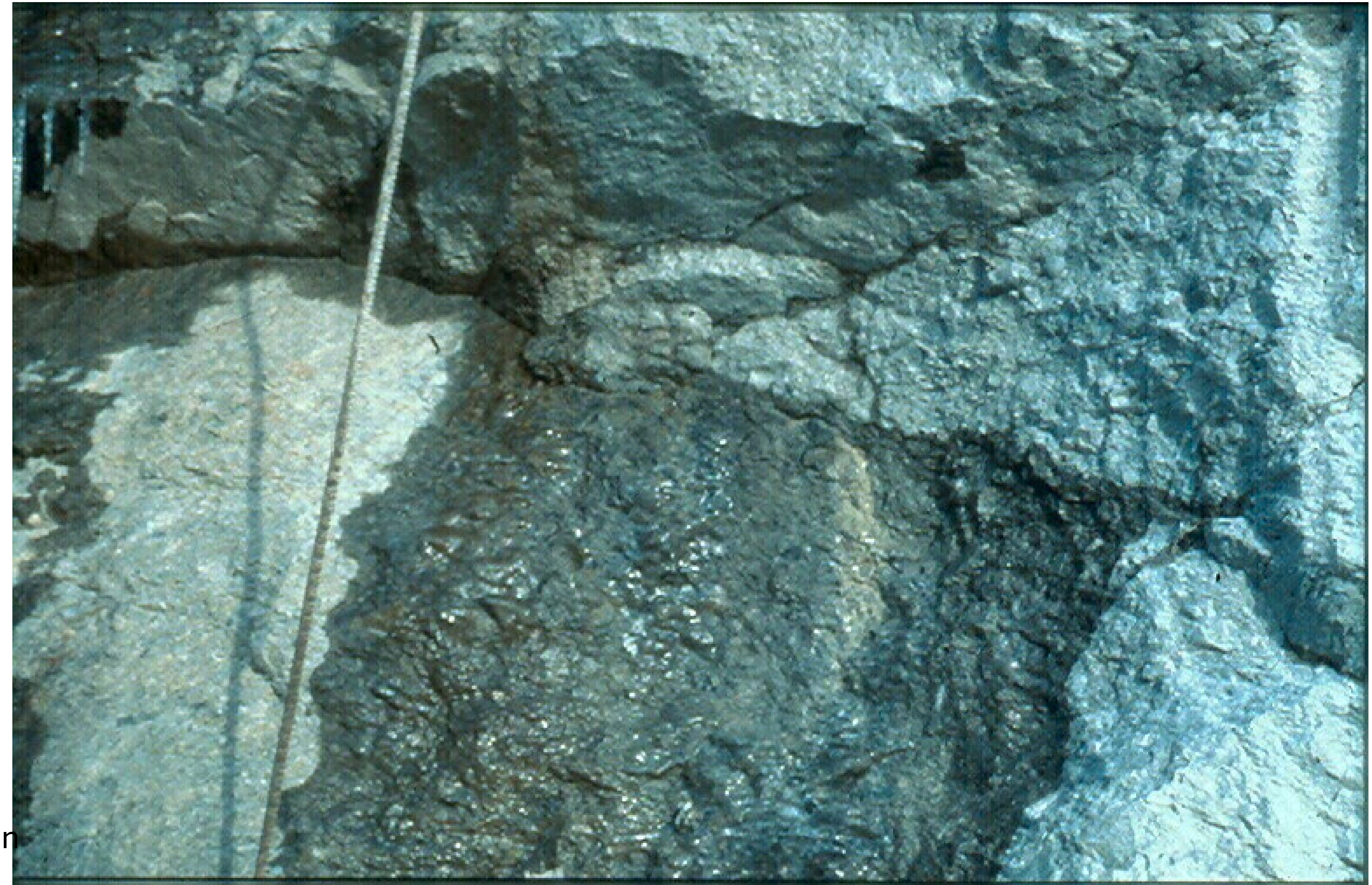

Fracture System Geometry and Flow represented with Discrete Fracture Network (DFN) Models

GEOFRAC – Stochastic Fracture Pattern Model

Rita Sousa, Violeta Ivanova , Wei Li

GEOFRAC's stochastic processes are implemented and optimized in MATLAB.

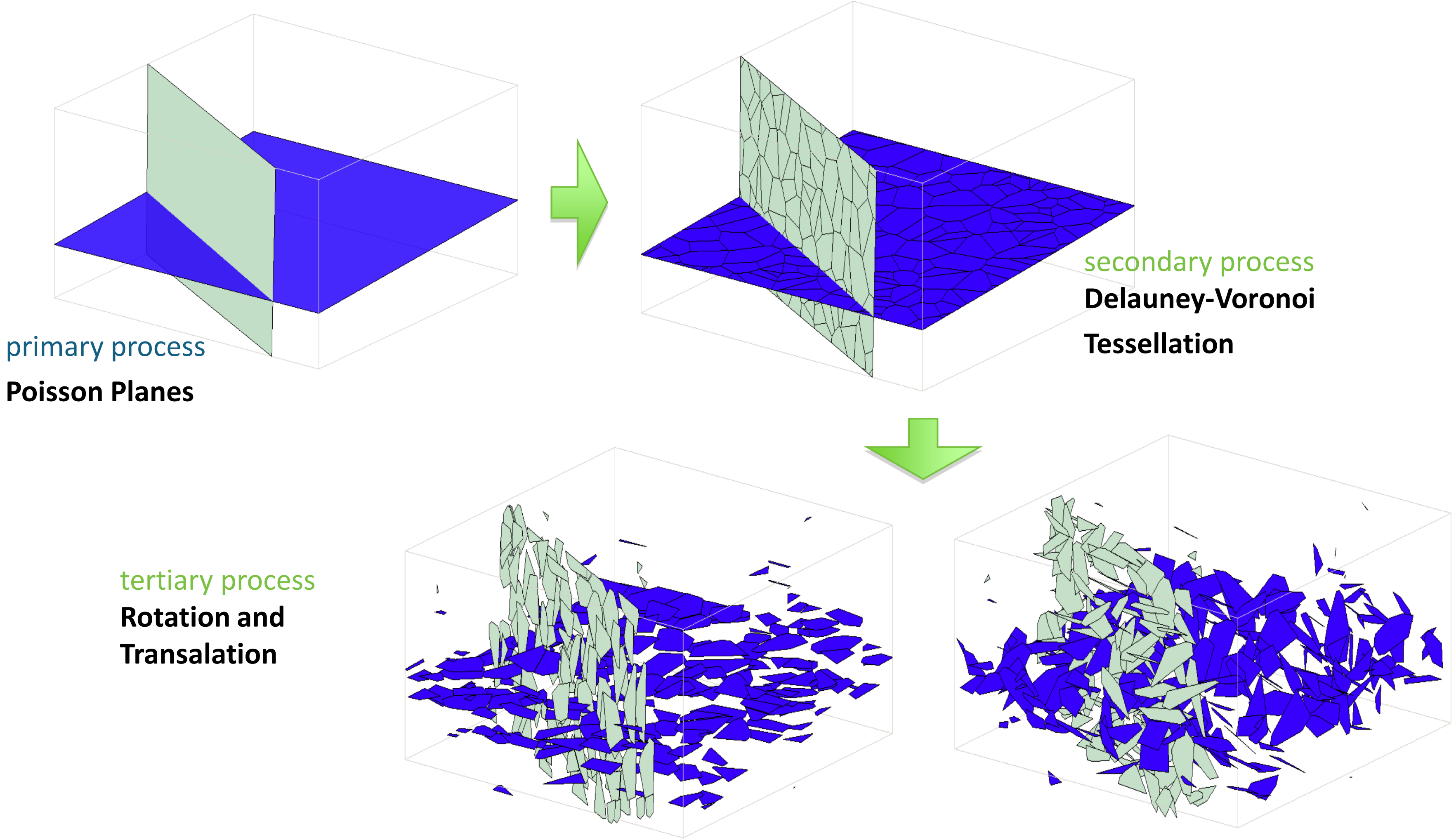

Fracture System Geometry and Flow represented with Discrete Fracture Network (DFN) Models

GEOFRAC – Flow Path and Intersection Process

FLOW-PATH CONTRIBUTING FRACTURES (two new algorithms)

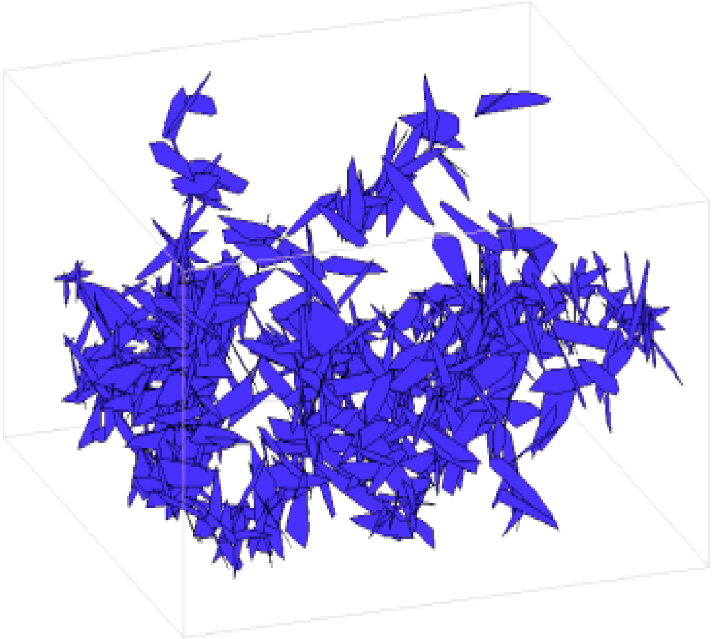

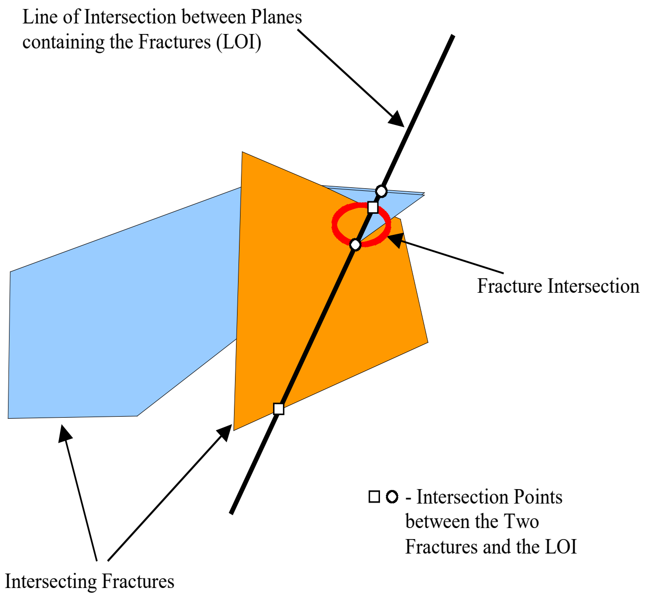

FRACTURE APERTURES: deterministic and probabilistic modeling of fracture thickness.

"CLEAN" FRACTURES: retaining only fractures that contribute to flow paths, i.e., those intersecting at least (1) two other fractures, or (2) a fracture and a boundary of the model.

HDR and EGS for Geothermal Energy Extraction - Basic Concepts

Modified from Jung, (2013)

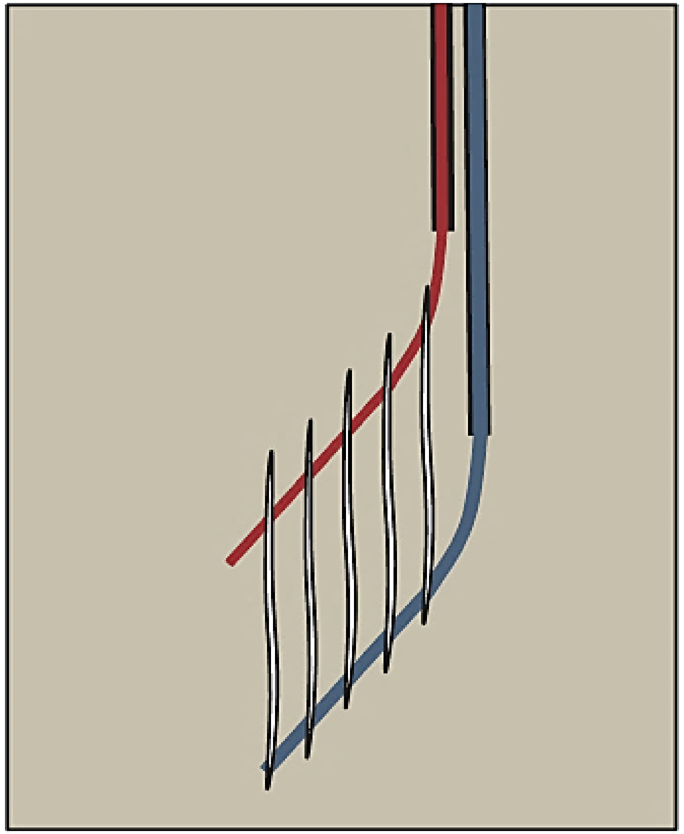

HDR-Concept

HDR (Hot Dry Rock) in "zero" permeability basement - creating fractures through **hydraulic fracturing**.

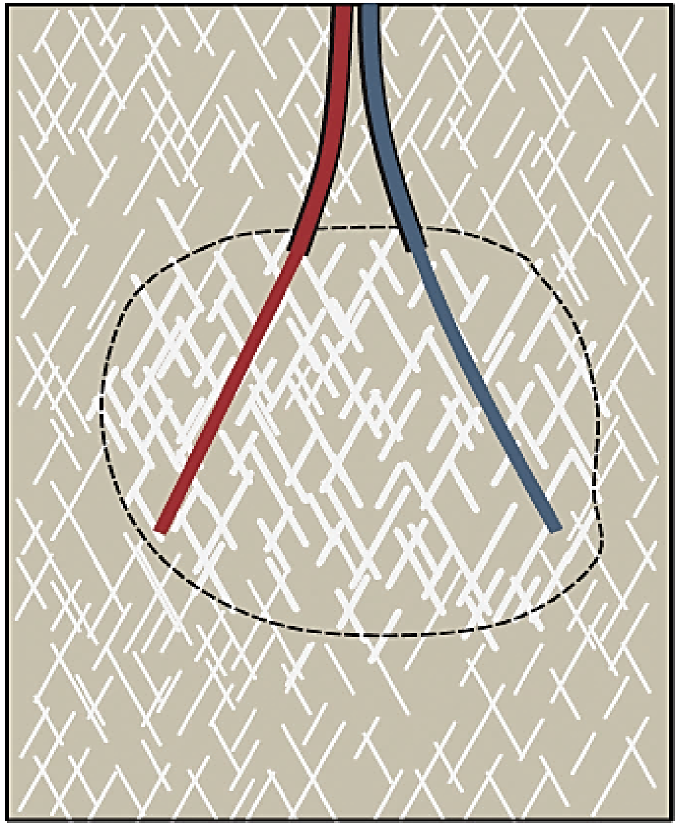

EGS-Concept

EGS (Engineered Geothermal Systems) **-enhancing** the existing fractured network through hydro-shearing

Fracture System Geometry and Flow represented with Discrete Fracture Network (DFN) Models

GEOFRAC – FLOW

FLOW PATH COMPUTATION

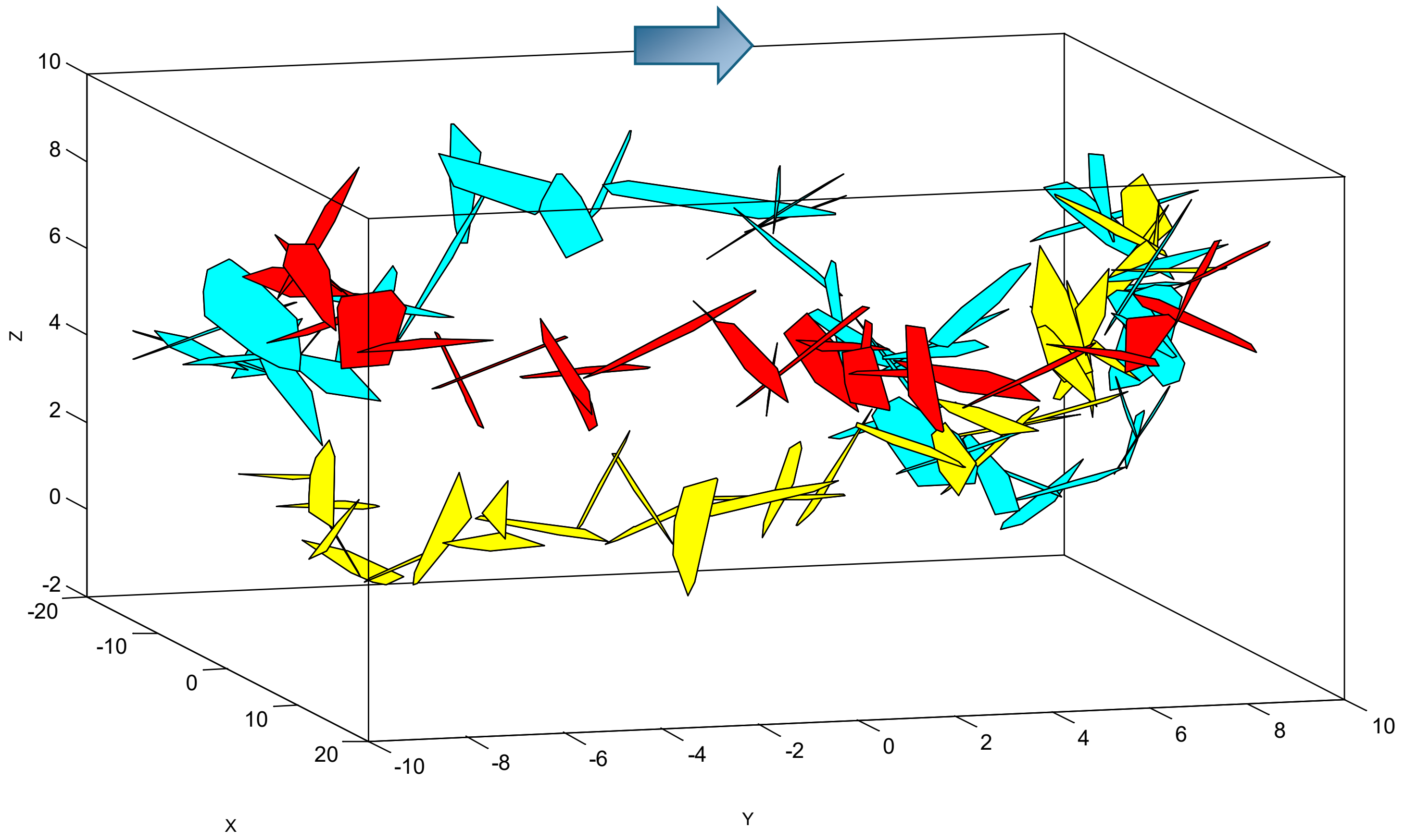

GEOFRAC – FLOW

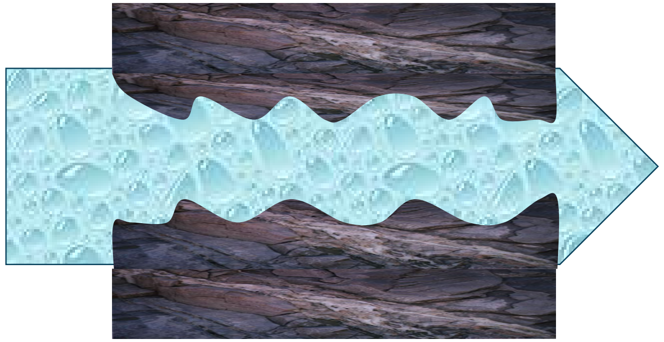

Model Assumptions

- Flow restricted to fractures (i.e. impervious rock)
- Laminar flow between parallel plates
- Fracture roughness (ε) taken into account through friction factor f
- Flow through most "likely" paths

Flow Rate (Parallel plates)

$$Q = \frac{wh^3 \Delta P}{12 f \mu \Delta L}$$

w: fracture width
h: aperture
ΔP: pressure gradient
μ: water dynamic viscosity
ΔL: fracture length

Fracture Roughness

$$f = 1 + 3.1\left(\frac{\varepsilon}{h}\right)^{1.5}$$

ε: fracture roughness
h : aperture

GEOFRAC – FLOW

Fracture Aperture Modeling

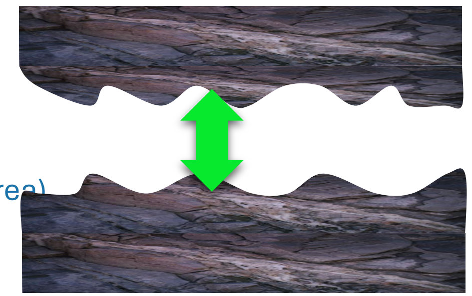

Deterministic Approach

$$h = \alpha 2 R_e^{\beta}$$

R_e : fracture polygon's equivalent radius (i.e., the radius of a circle with the same area)
h : fracture polygon aperture
α , β : coefficients that depend on the site's geology.

Probabilistic Approach

$$f_{TR}(h) = \frac{f(h)}{\int_{h_{\min}}^{h_{\max}} f(h)\,dh} \qquad h_{\min} \le h \le h_{\max}$$

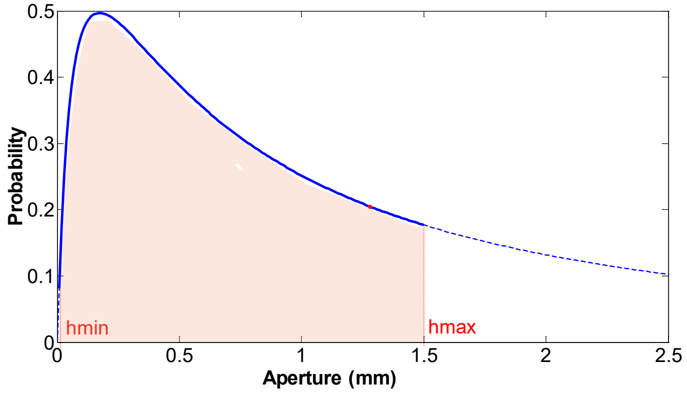

h_{min}, h_{max} : lower and upper limit
f (h) : lognormal distribution of the aperture, h, with parameters μ and σ.

$$f(h) = \frac{1}{h\sigma\sqrt{2\pi}} \exp\left(\frac{-(\ln h - \mu)^2}{2\sigma^2}\right), \quad 0 \le h \le \infty$$

Fracture System Geometry, Flow and Temperature represented with Discrete Fracture Network (DFN) Models

GEOFRAC-THERMAL

The heat transfer problem can be treated as heat transfer between flow and two parallel isothermal plates.

$$T_2 = T_r - (T_r - T_1)\exp(-\frac{h_T PL}{\dot{m}C_P})$$

$$h_T = \frac{Nu \times k_f}{D_h}$$

$$\overline{Nu_{D_h}} = 7.54 + \frac{0.03(D_h/L)Re_{D_h}Pr}{1 + 0.016[(D_h/L)Re_{D_h}Pr]^{2/3}}$$

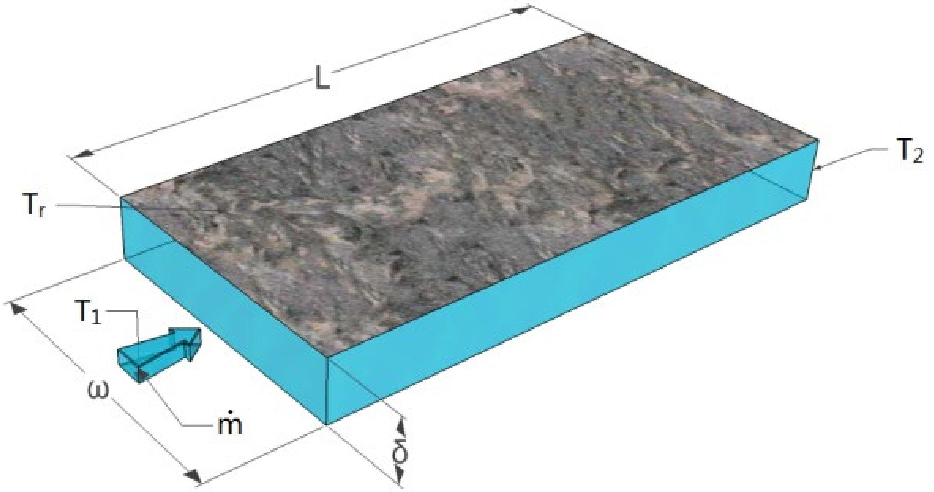

P is perimeter 2(δ+w);
is the mass flow rate;
k_f is the fluid heat conductivity
D_h is the hydraulic diameter of the conduct

h_T is heat convection coefficient;
L is the fracture length;
Nu is the Nusselt number
C_p is the specific heat capacity

GEOFRAC Flow and Thermal

Flow Rate in each link –Temperature at each node

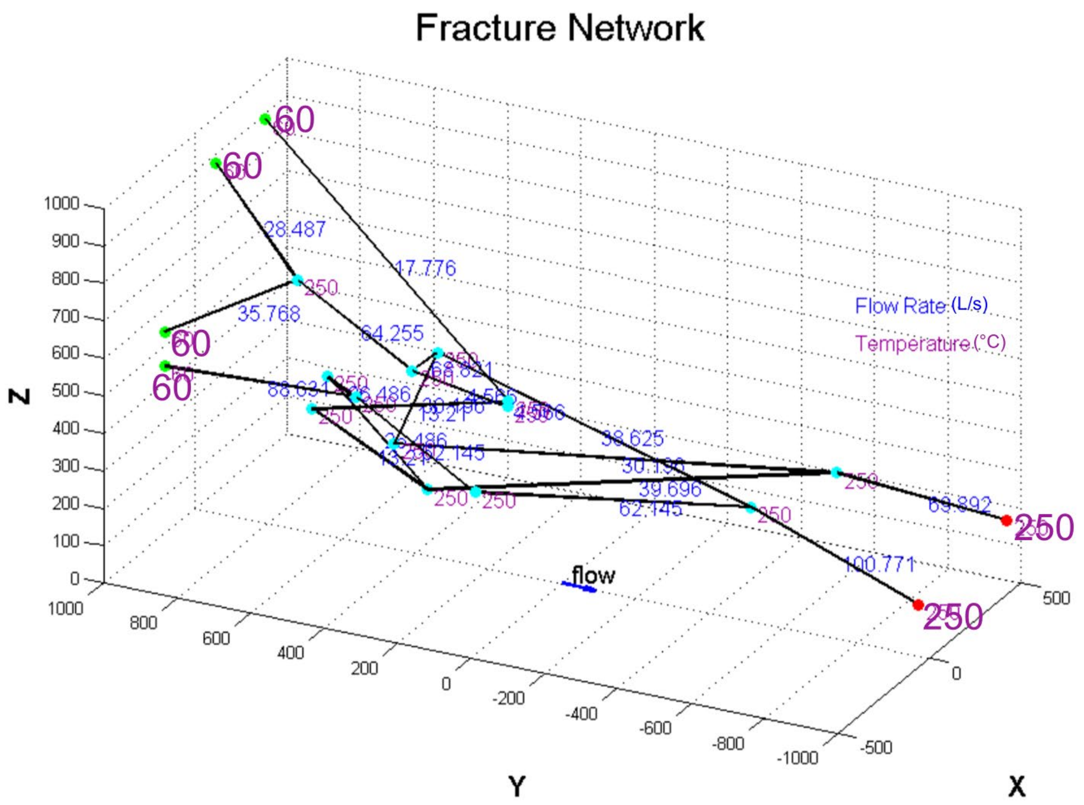

Block 2000 x 1000 x 1000 m - Rock Temperature 250 ^{o}C

Thermal Drawdown Problem

Example:
During the Fenton Hill Project, a full-scale operation of the loop occurred from January 27 to April 13, 1978 (75 days in total) (Tester and Albright, 1979).

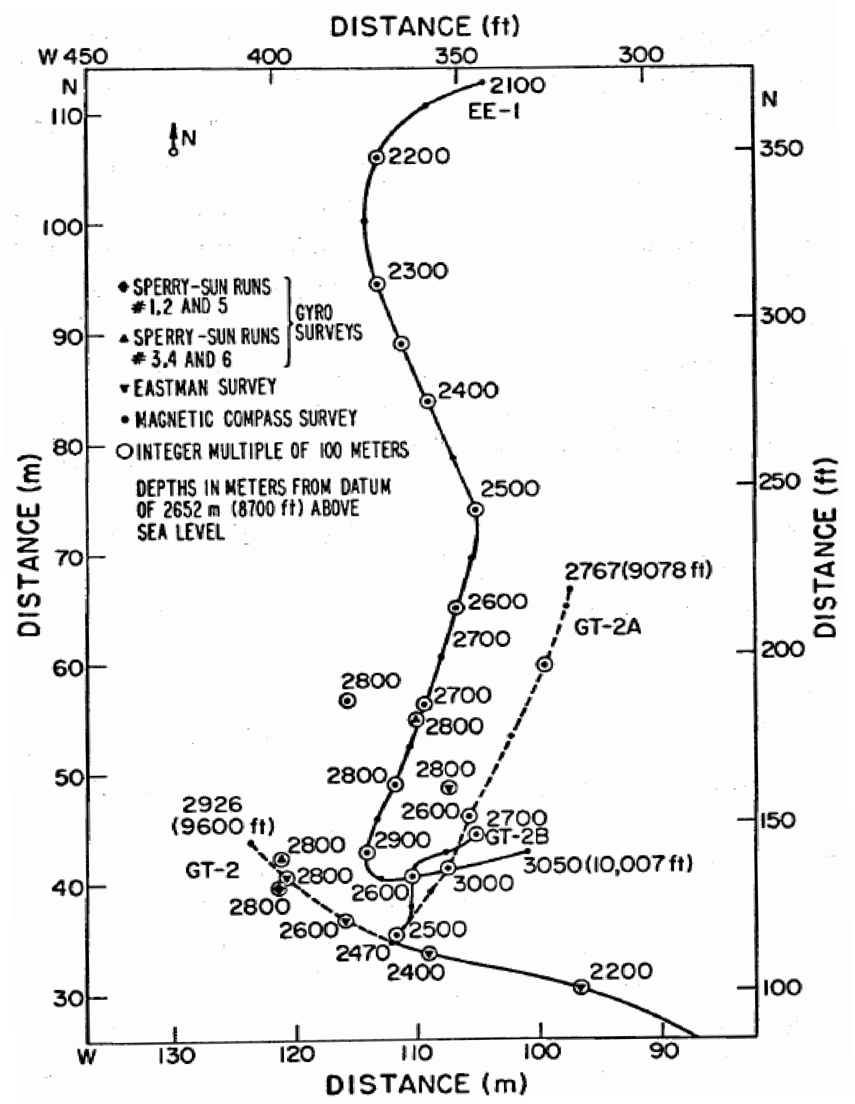

Thermal Drawdown Problem

The thermal drawdown of the Fenton Hill geothermal reservoir predicted by our thermal drawdown model matched the measurement.

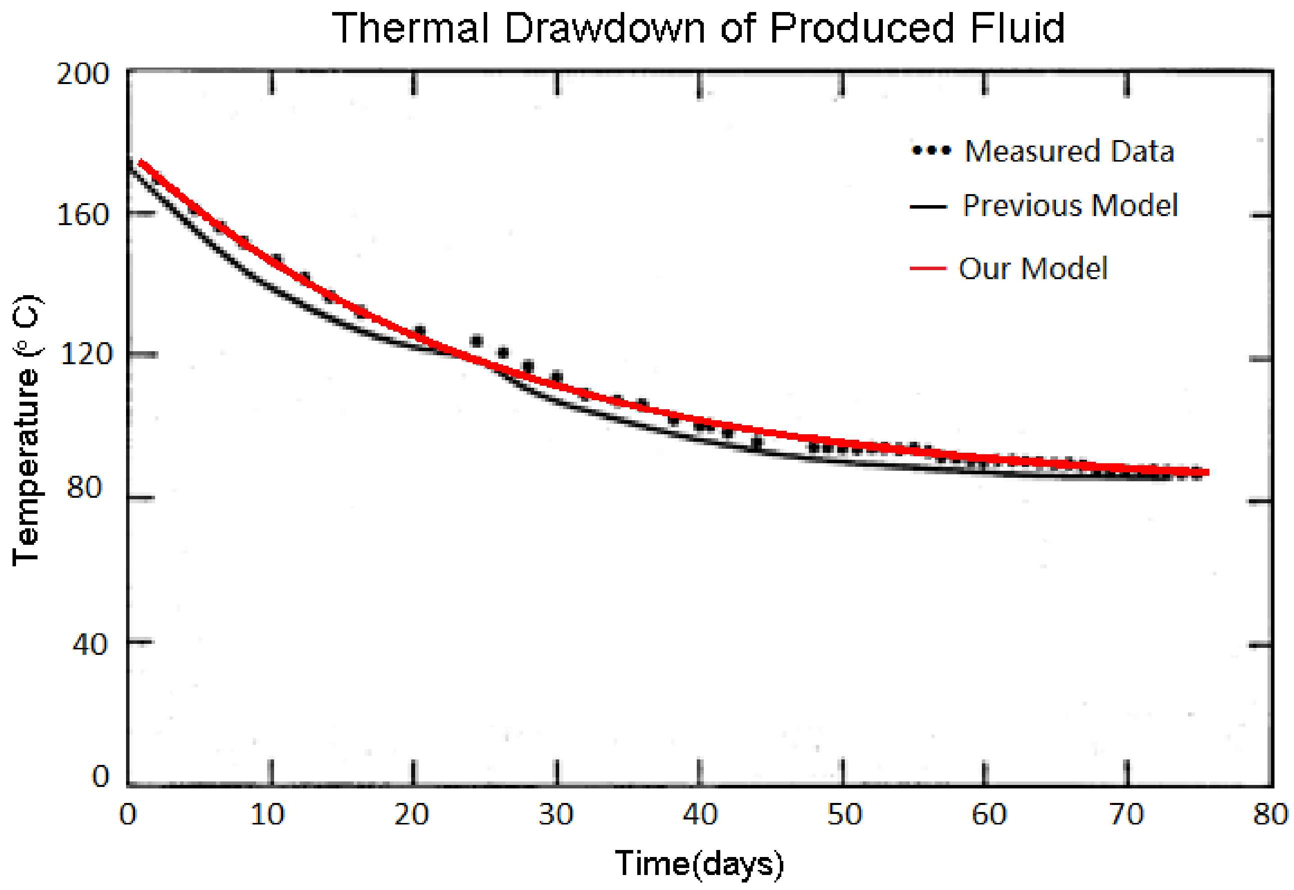

Mechanics of In-situ Leaching

Background and Introduction

Discrete Fracture Network **-**

GEOFRAC/GEOFRAC FLOW/GEOFRAC THERMAL

Fracture Flow and Transport

Hydraulic Fracturing

Dissolution

Conclusions

FLOW EXPERIMENTS WITH HELE-SHAW CELL

PhD Thesis Villamor Lora

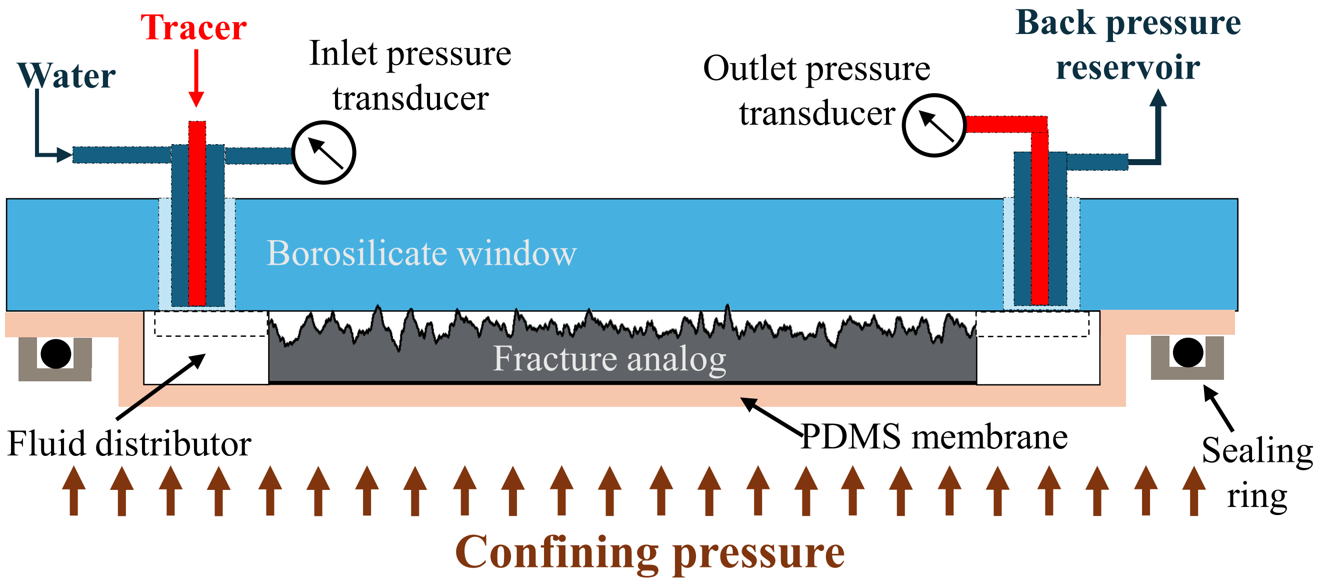

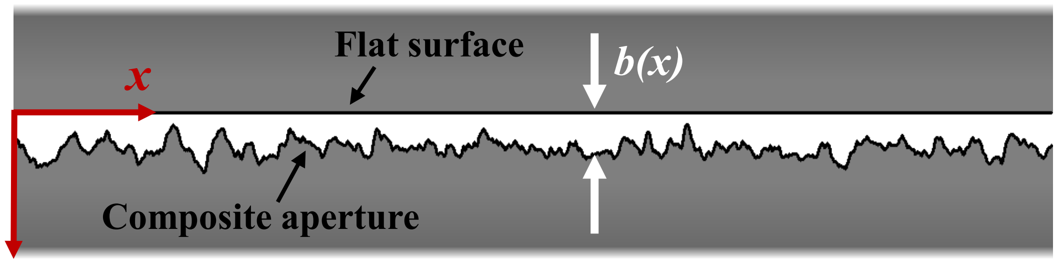

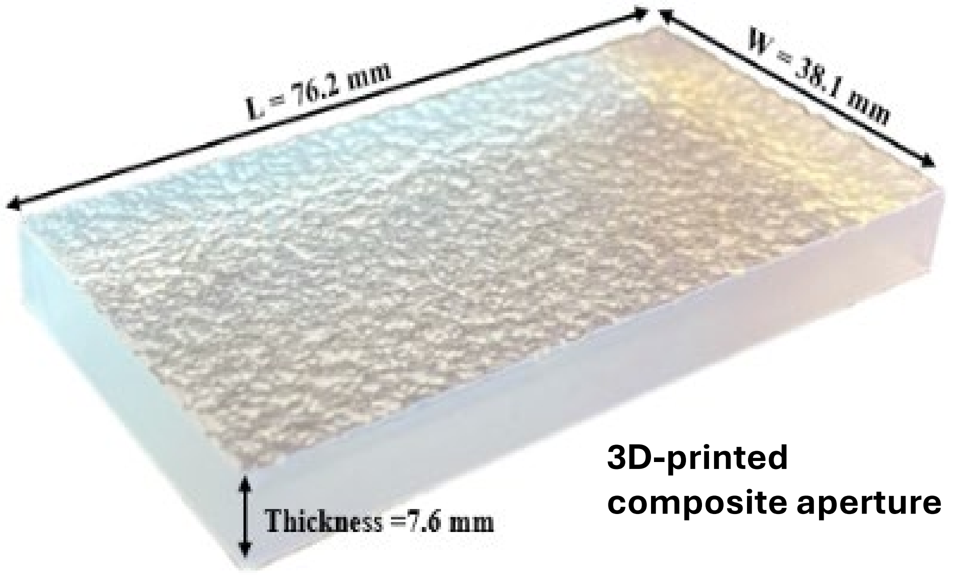

3D-printed composite aperture

PRESSURE-CONTROLLED HELE-SHAW CELL

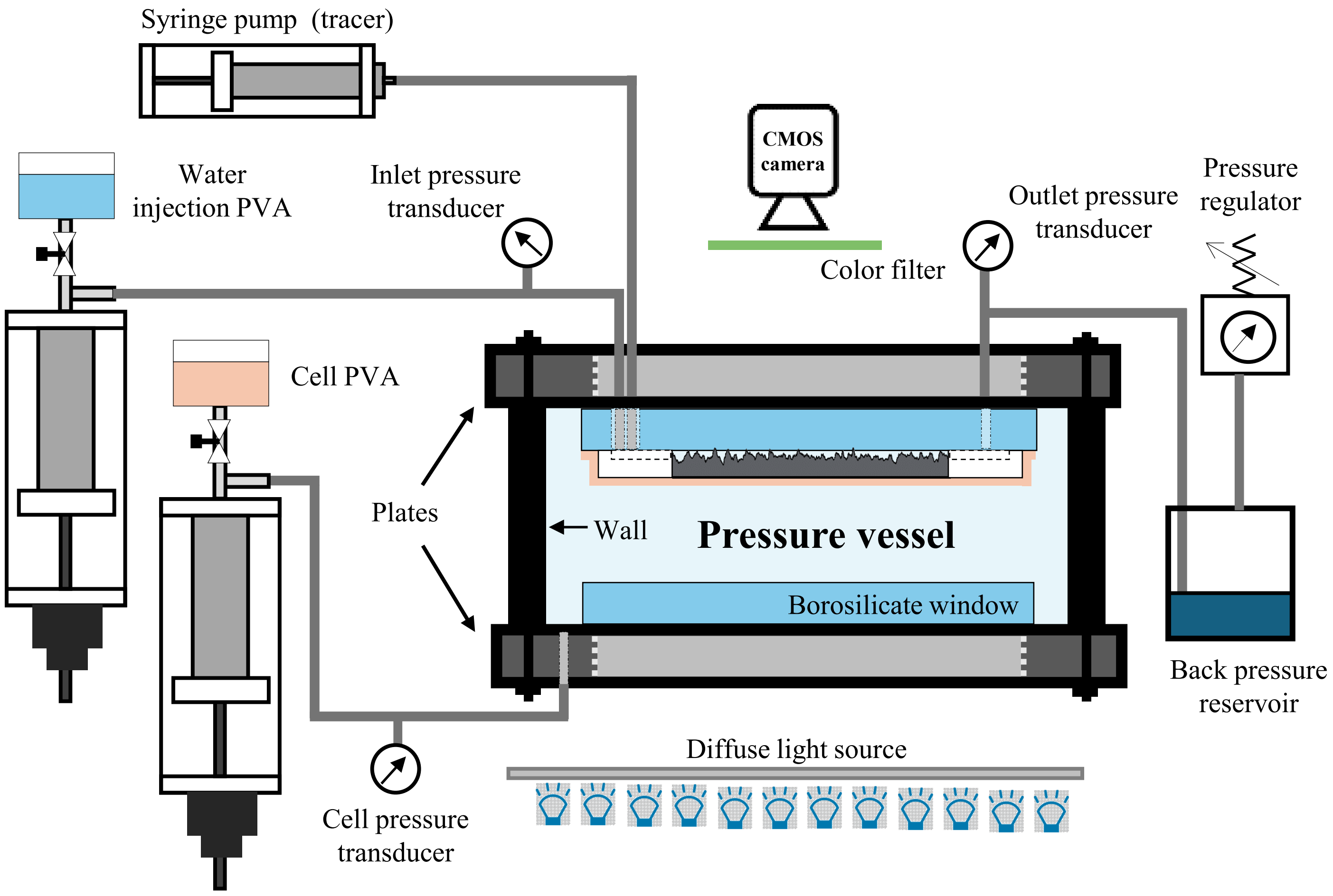

Lab-Field scaling

$$\sigma_{lab} / E_{lab} \sim \sigma_{field} / E_{field}$$

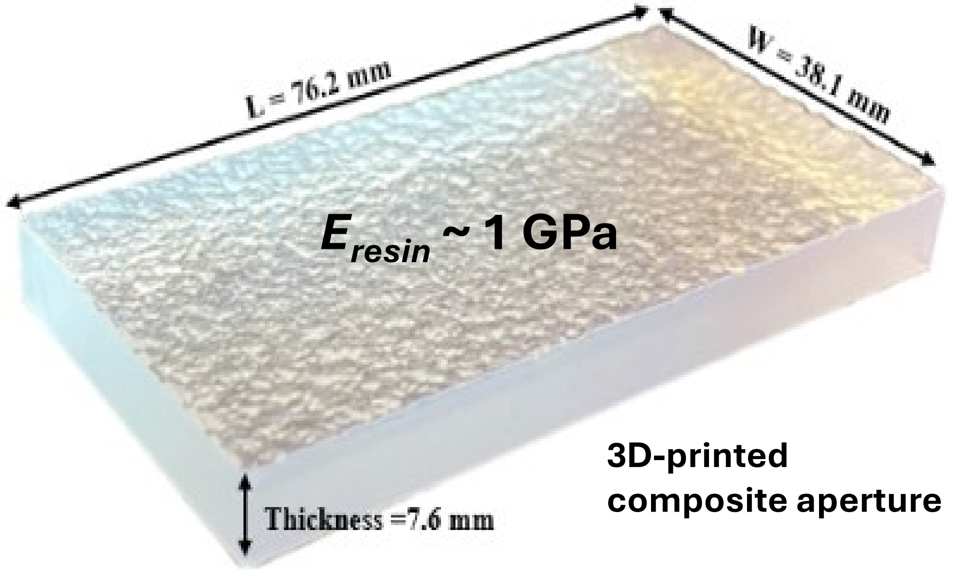

3D-printed composite aperture

Fracture deformation and Pressure-dependent permeability

FRACTURE DEFORMATION

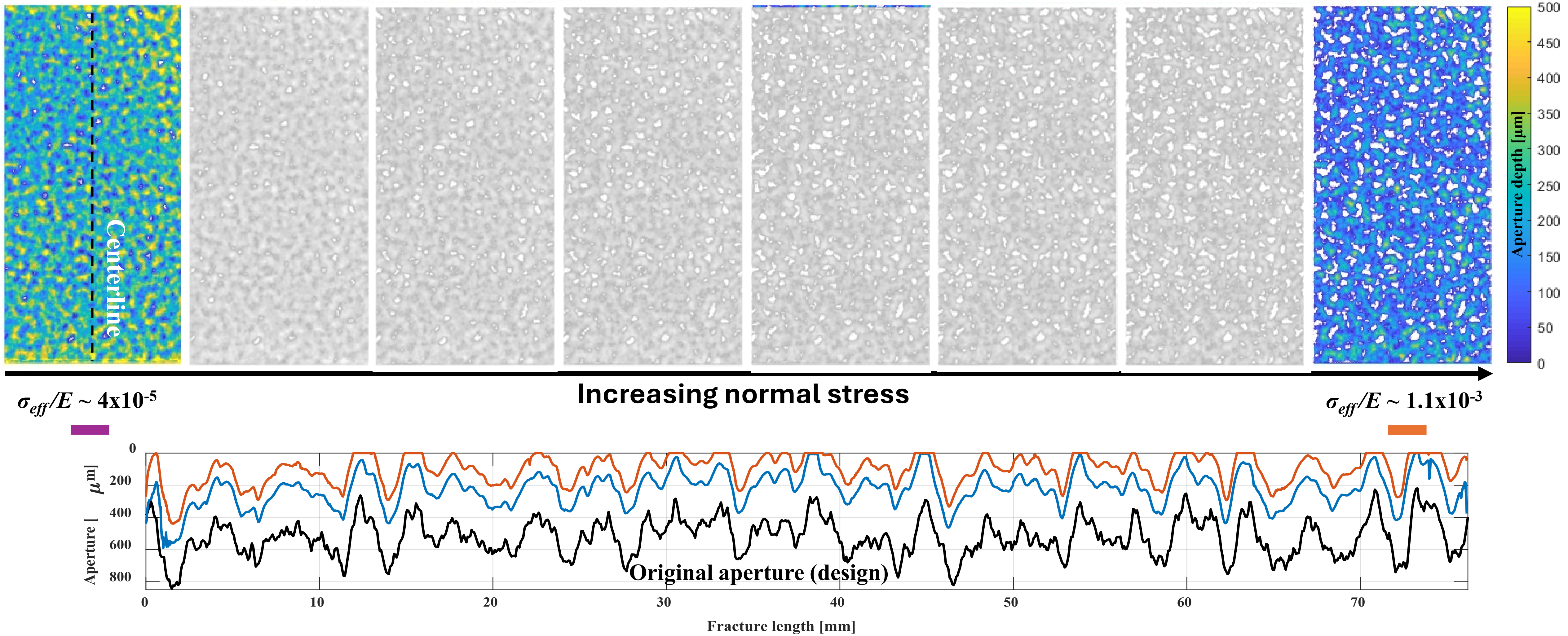

DETERMINATION OF THE FLOW FIELD SIMULATION

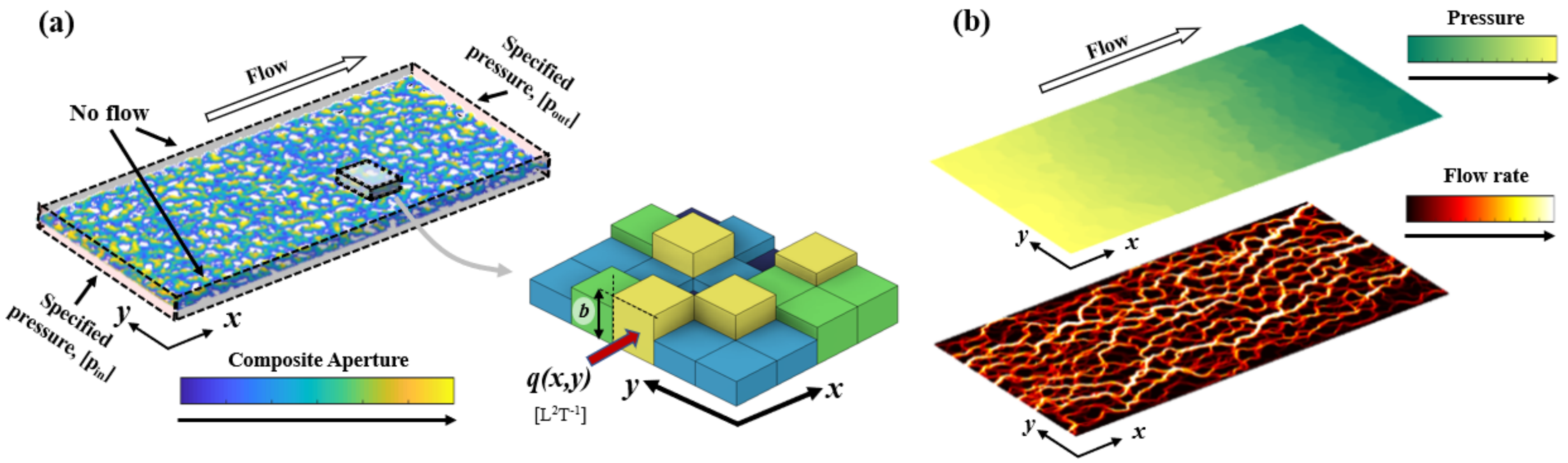

Increasing normal stress

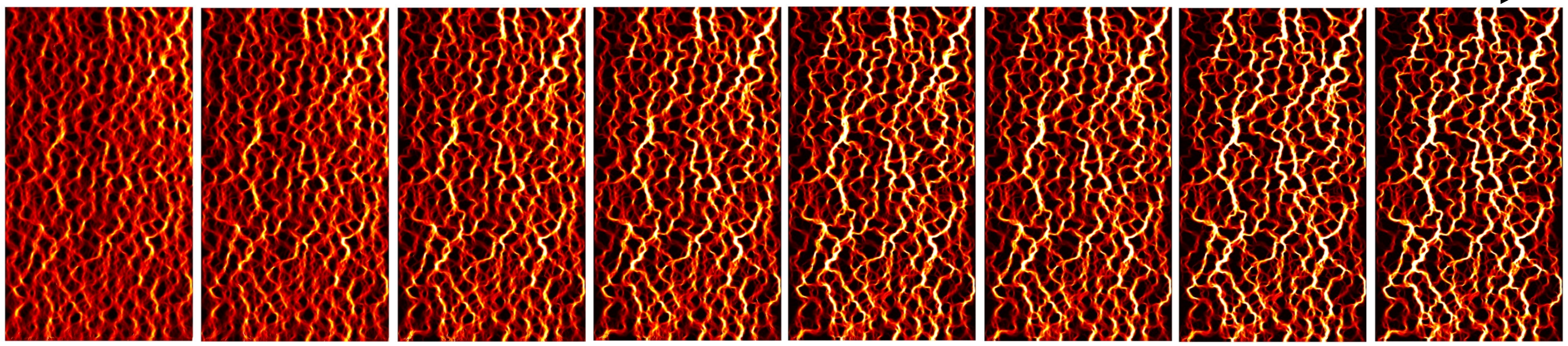

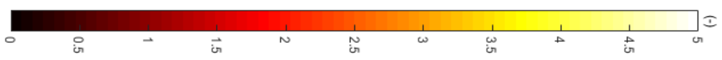

$$q_{ij}/\overline{q}_x = \frac{q_{ij}}{Q_{in}/n_y}$$

Simulations vs. Experiments

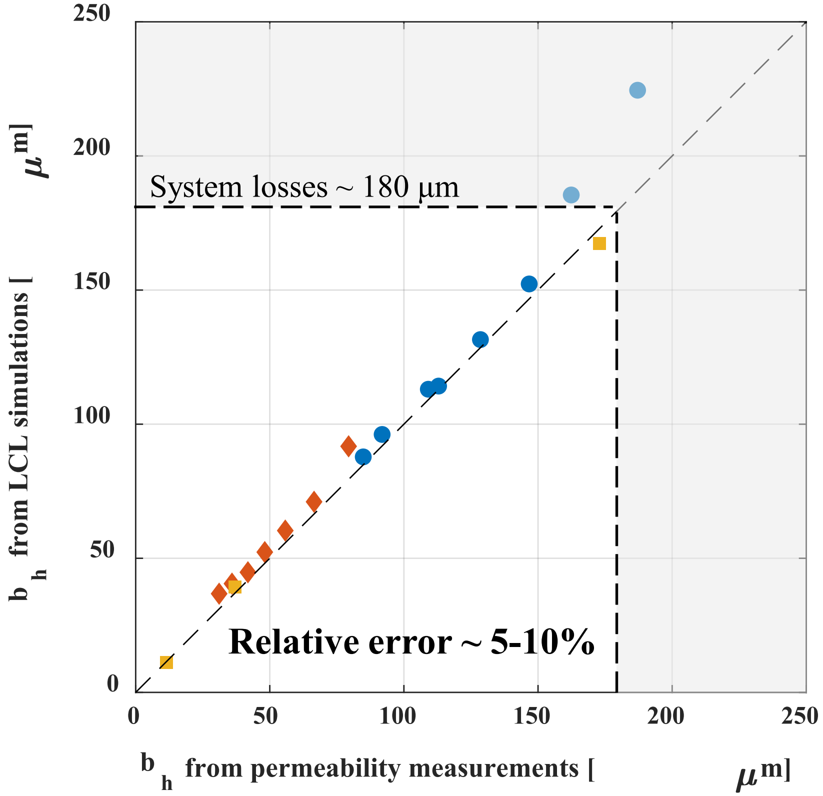

Hydraulic aperture

$$b_h = \sqrt[3]{12\mu \frac{Q}{\Delta P} \frac{L}{W}}$$

INJECT DYE AND OBSERVE CONCENTRATION

2D CONCENTRATION MAPS

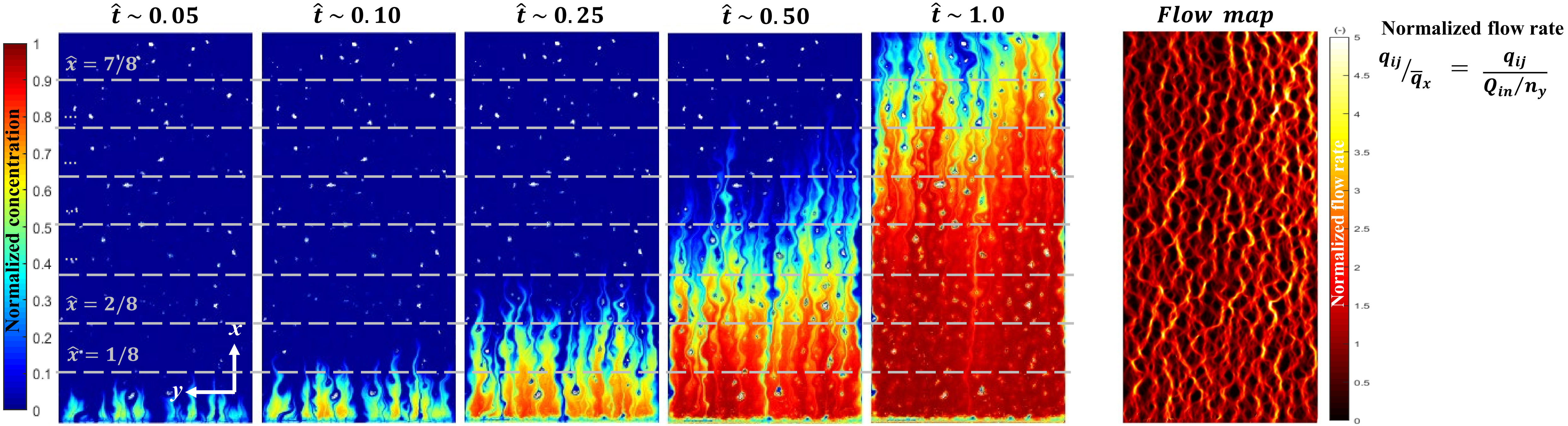

Dimensionless time

$$\hat{t} = \frac{t\,Q}{pVol}$$

Dimensionless concentration

$$\hat{C} = \frac{C}{C_0}$$

Dimensionless position

$$\hat{x} = \frac{x}{L}$$

Flux-averaged concentration

$$\hat{C} = \frac{\sum_{i=1}^{n} C_i \cdot q_i}{\sum_{i=1}^{n} q_i}$$

PARTICLE TRACKING SIMULATIONS

Concentration maps

Flow maps

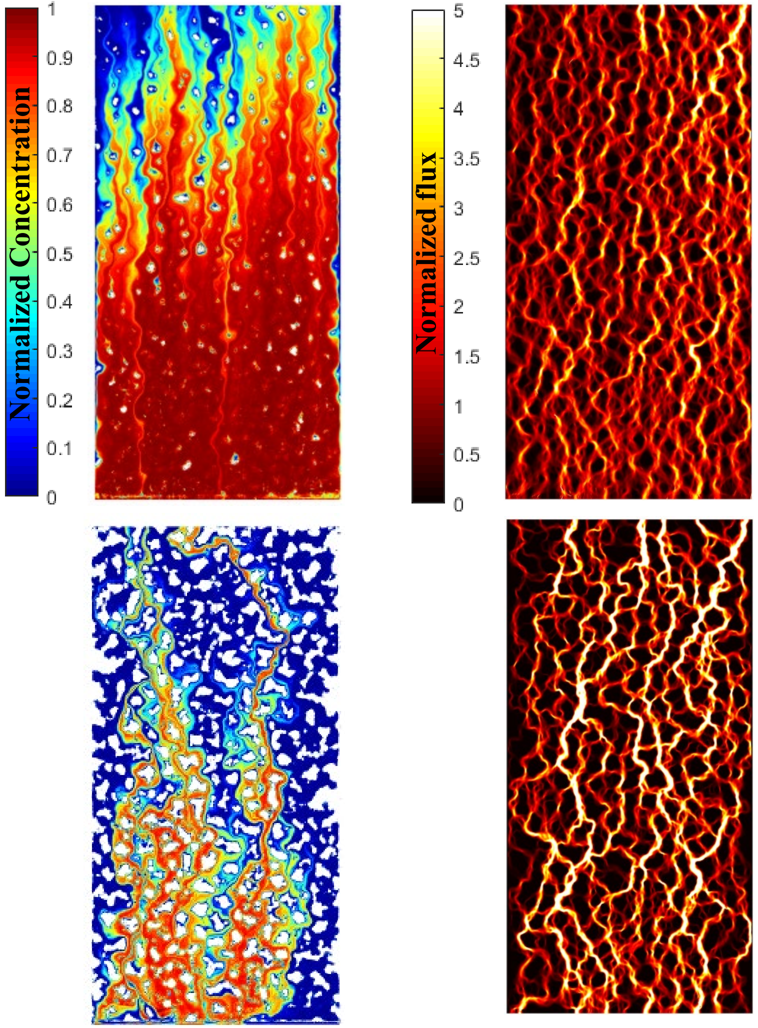

Uniform velocity

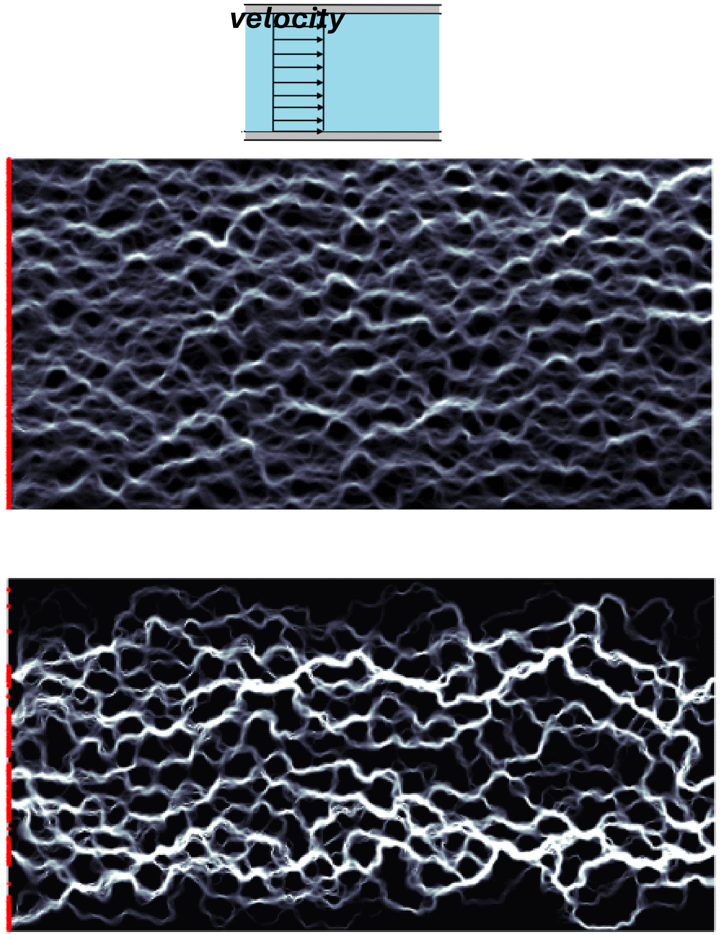

Parabolic

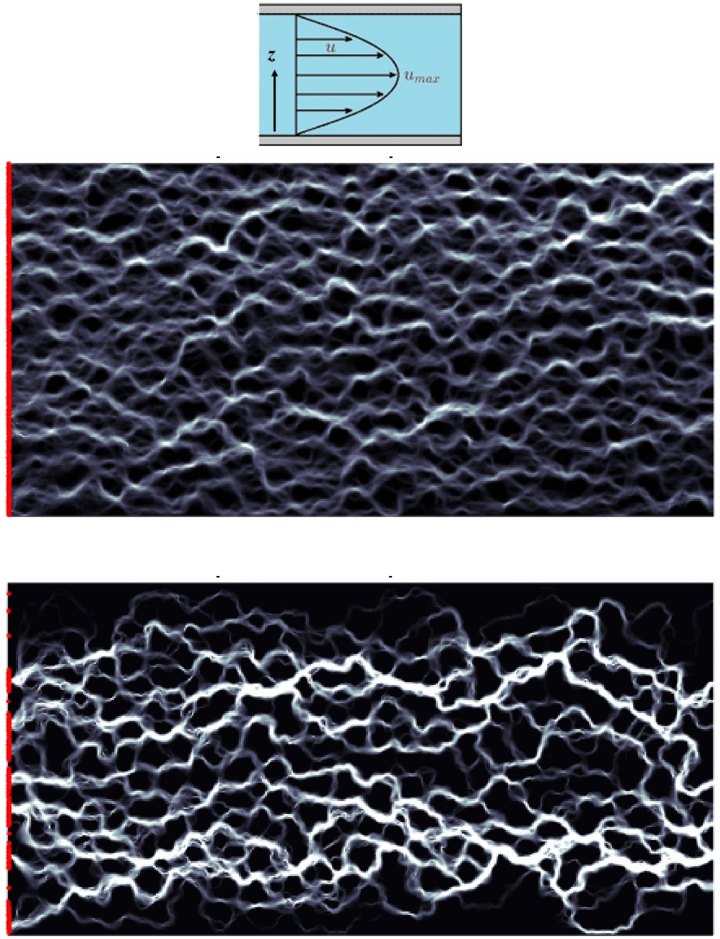

Mechanics of In-situ Leaching

Background and Introduction

Discrete Fracture Network **-**

GEOFRAC/GEOFRAC FLOW/GEOFRAC THERMAL

Fracture Flow and Transport

Hydraulic Fracturing

Dissolution

Conclusions

HDR and EGS for Geothermal Energy Extraction - Basic Concepts

Modified from Jung, (2013)

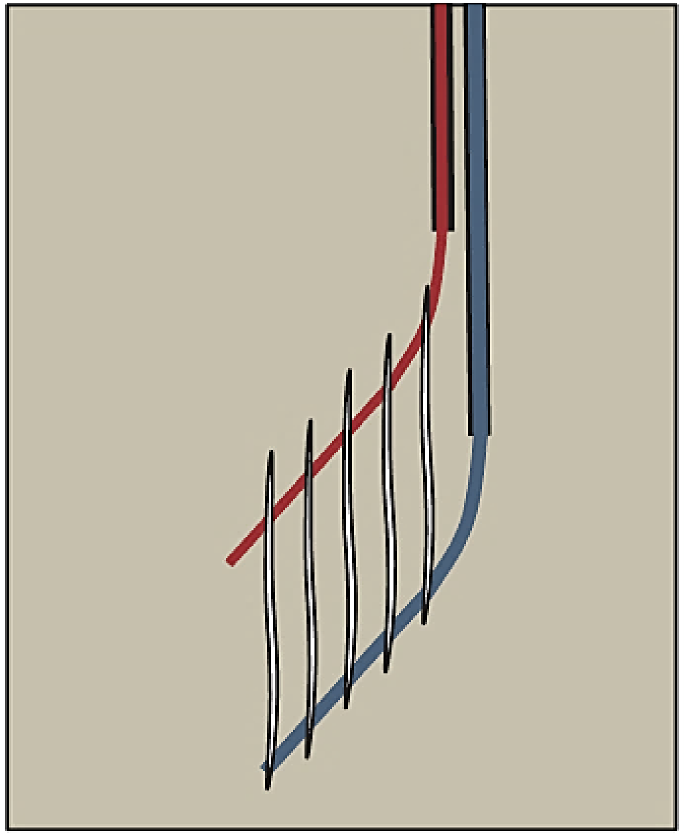

HDR-Concept

HDR (Hot Dry Rock) in “zero” permeability basement - creating fractures through **hydraulic fracturing**.

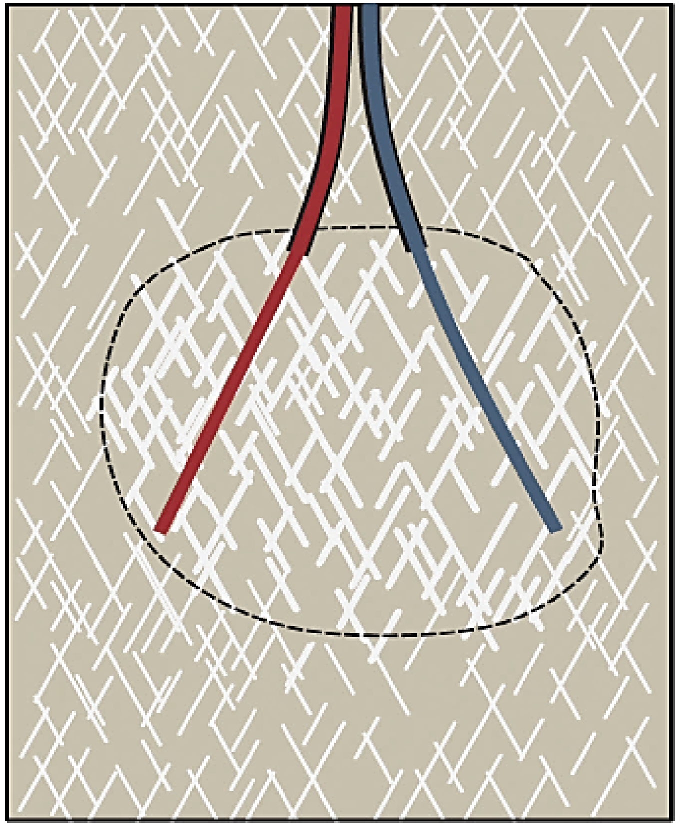

EGS-Concept

EGS (Engineered Geothermal Systems) **-enhancing** the existing fractured network through hydro-shearing

SCHEMATIC OF TESTING
Prismatic Specimens with Pre-existing Fractures – "FLAWS"
Specimen dimensions, number and orientation of flaws vary

PhD Theses Omar AlDajani, Bing Li

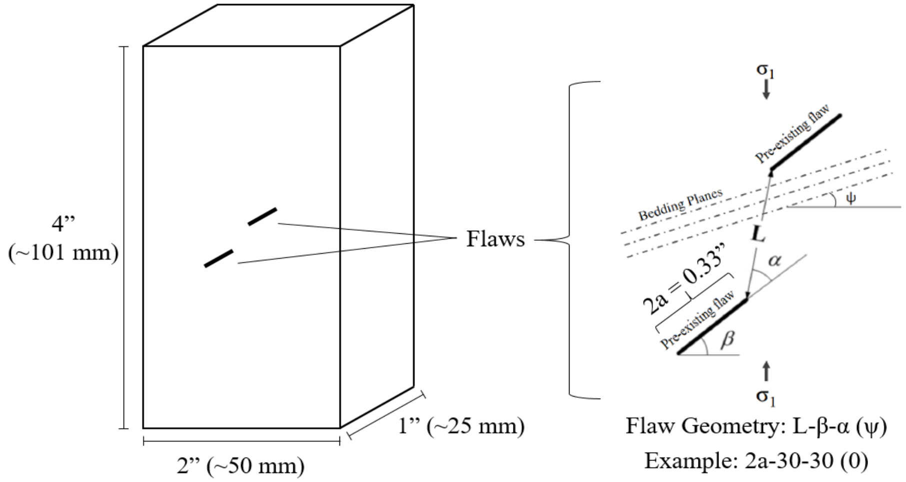

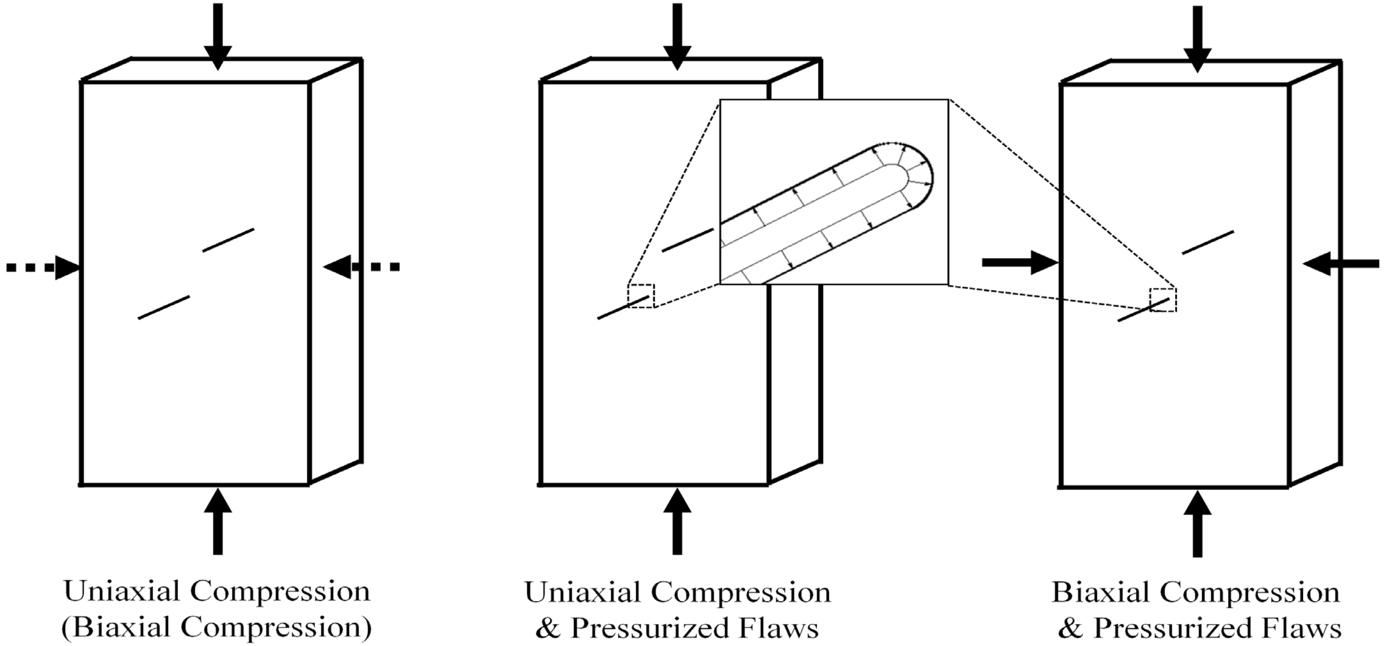

Hydraulic Fracturing Tests

Test Setup – Overall View

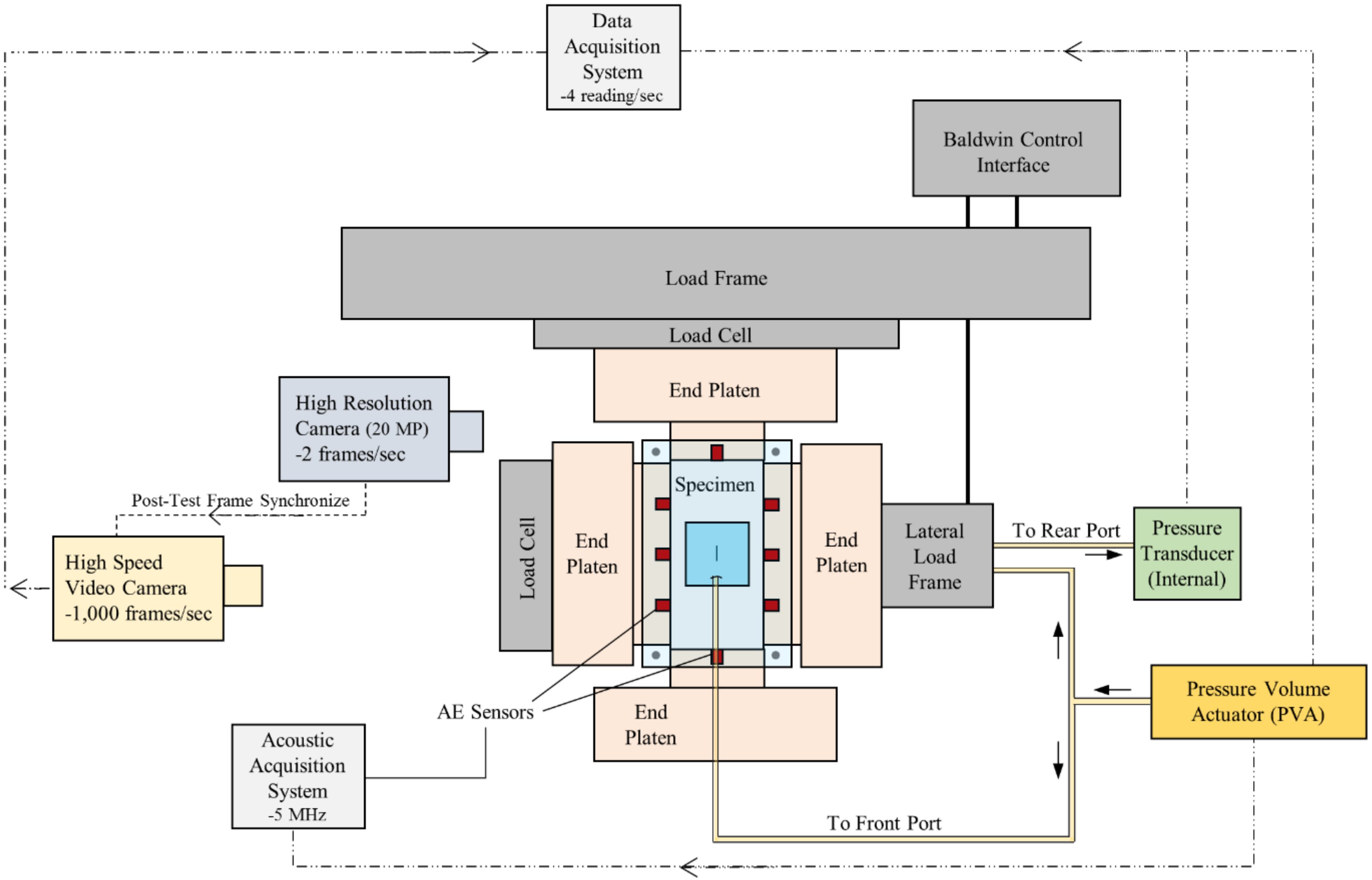

Hydraulic Fracturing Tests

Test Setup – Overall View

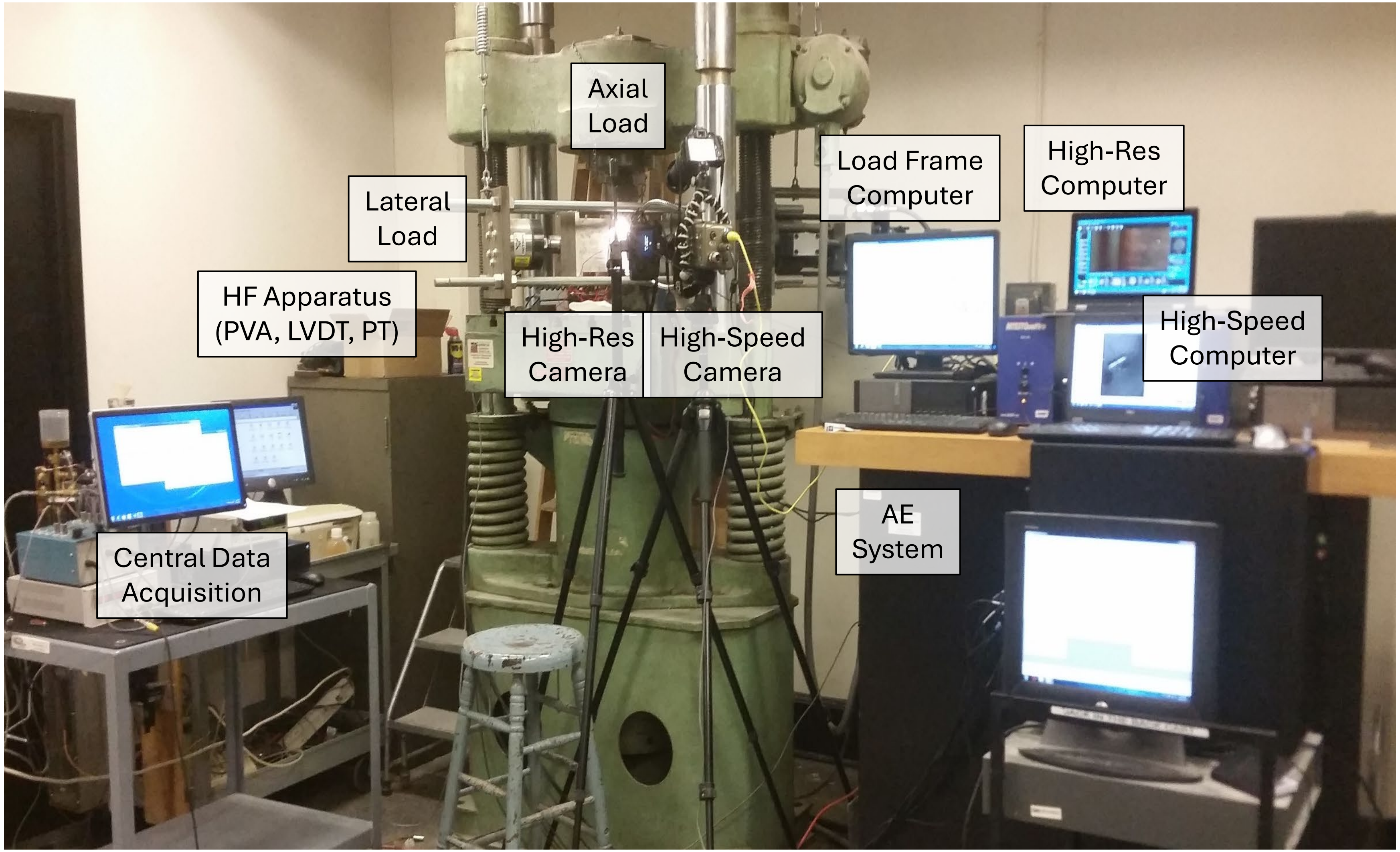

Hydraulic Fracturing - Present Pressurization Device

Uniaxial

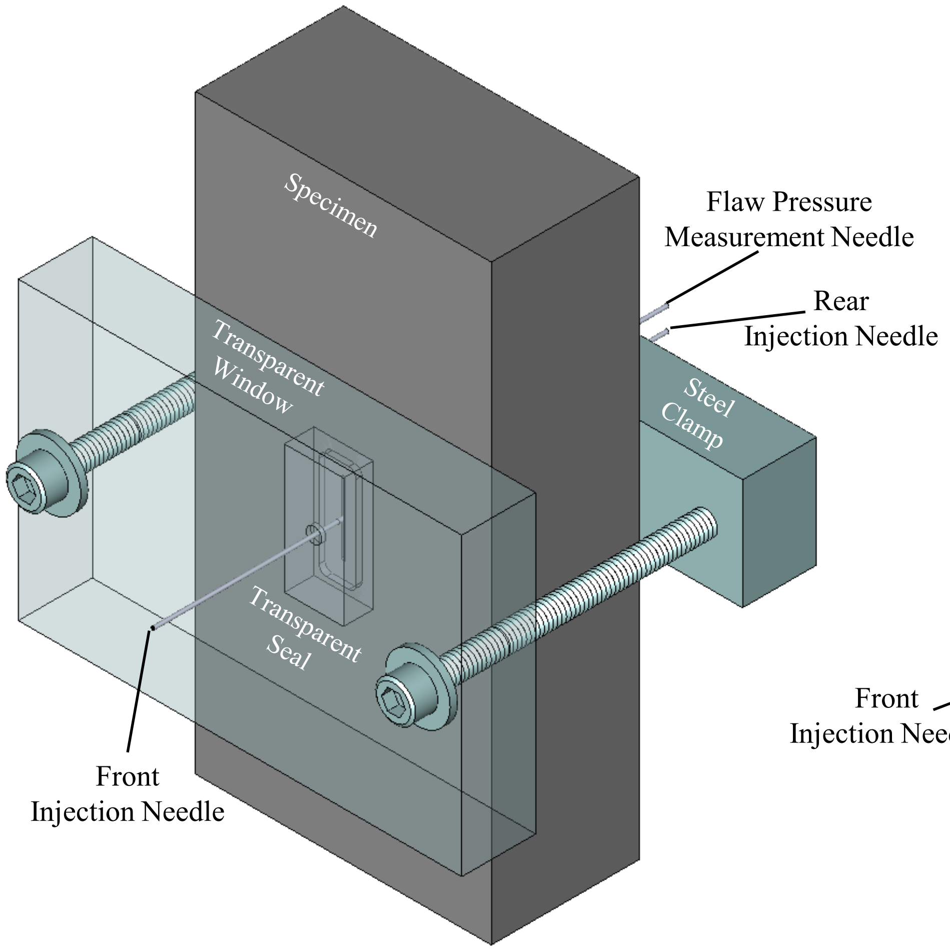

Biaxial

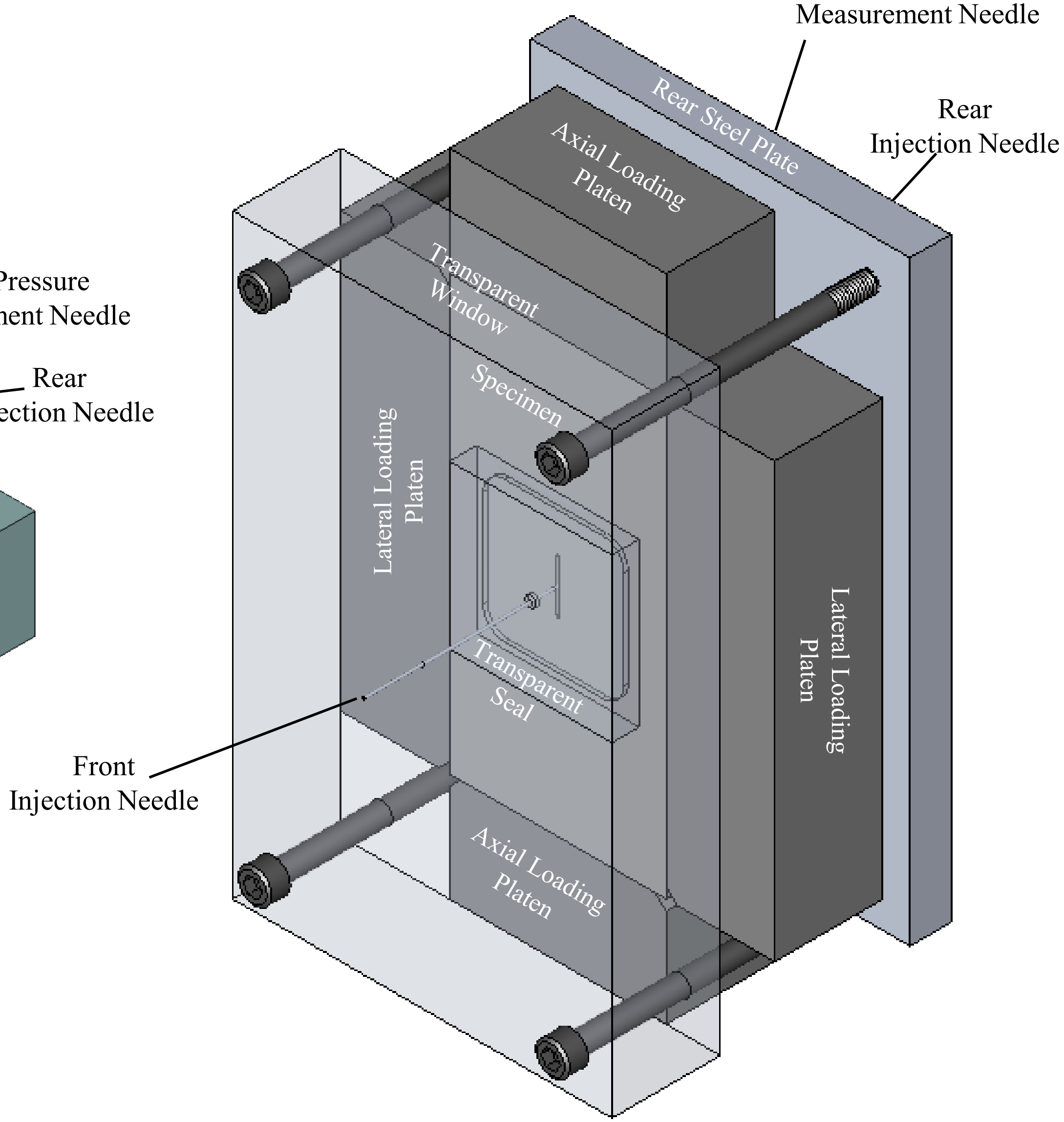

Pressure/Volume – Time Behavior in Hydraulic Fracturing Test

Entire Test

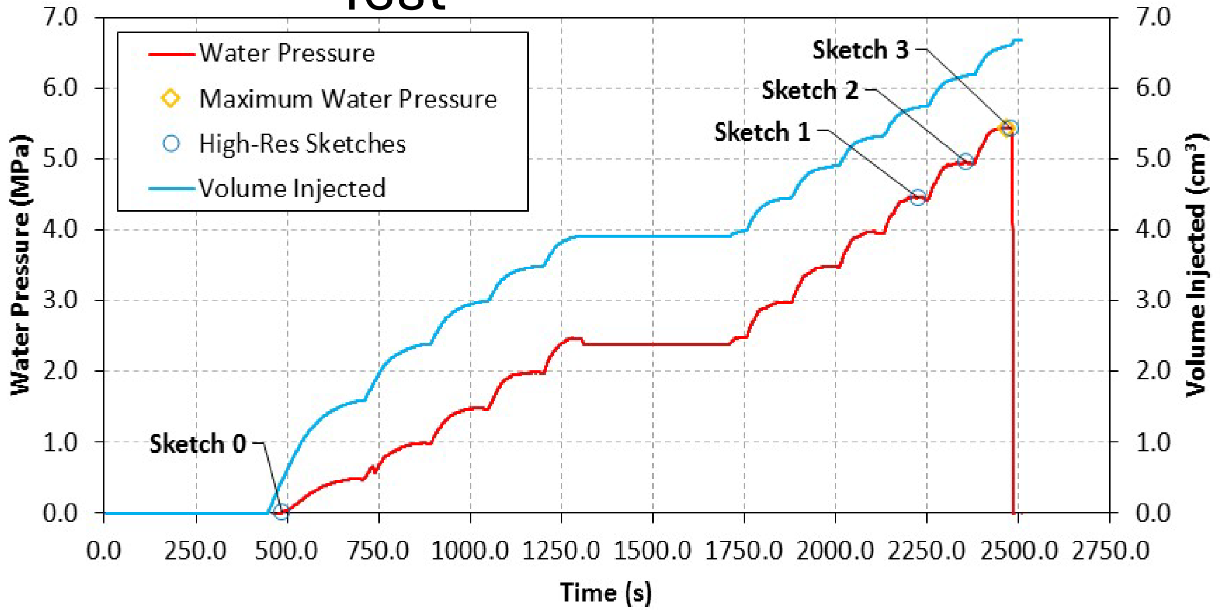

Final Stage

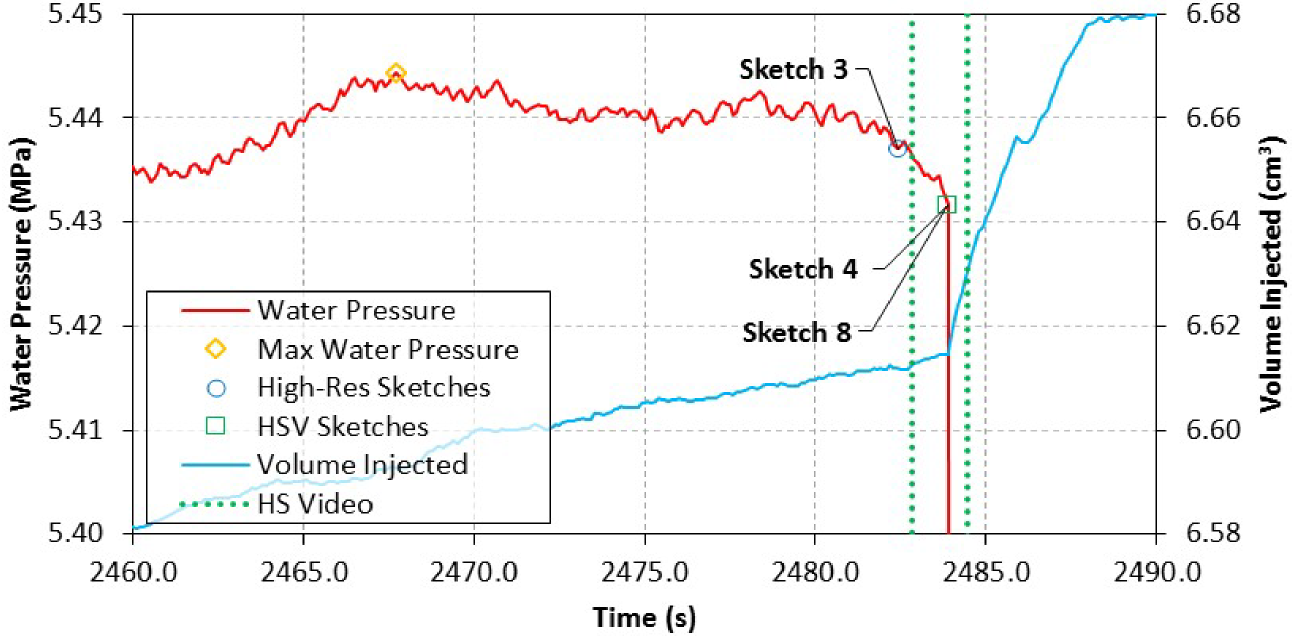

Visual Observations in Hydraulic Fracturing Test

Sketch 0

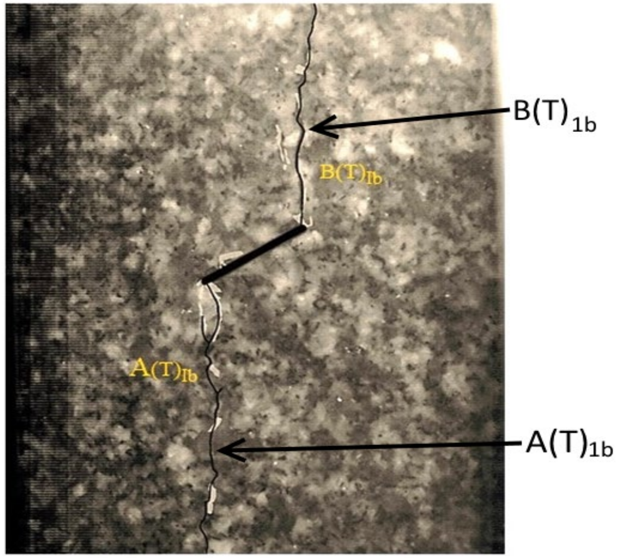

Sketch 8

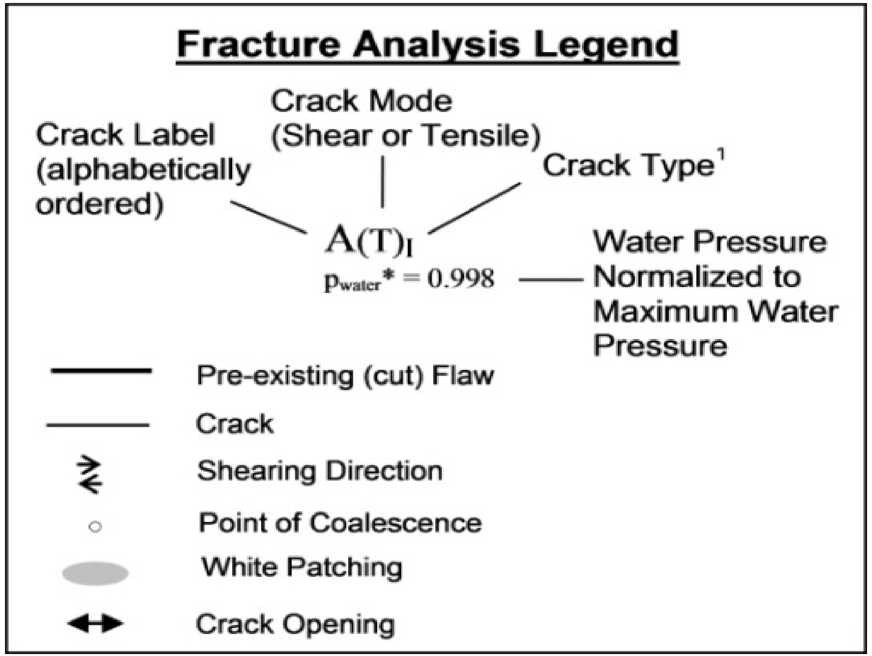

Visual Observations in Hydraulic Fracturing Test

Sketch 6

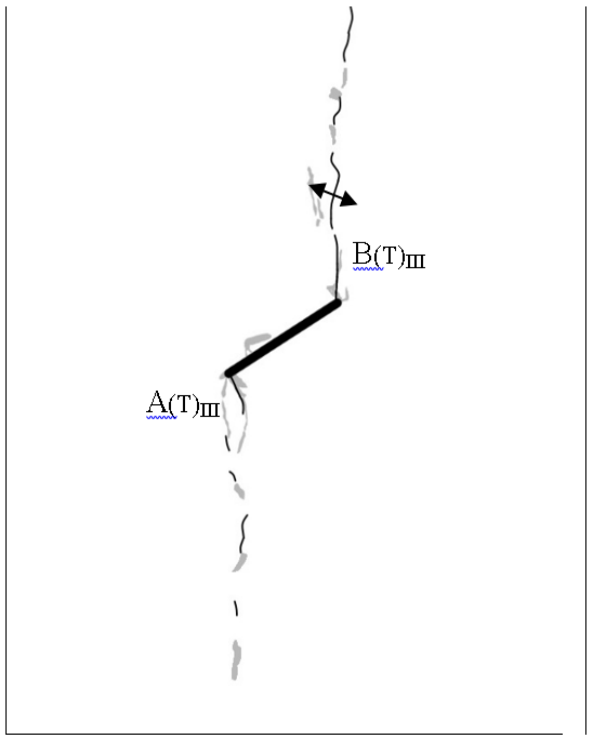

HSV **frame**:	-7673
Time:	41 min – 23.89253 sec
$\mathbf{p_{water}}$:	5.43 MPa
$\boldsymbol{\sigma_{vertical}}$:	5.0 MPa

Tensile crack $B(T)_{III}$ opens and propagates further through the linkage and extension of the existing segments.

Hydraulic Fracturing Tests on Granite(left) and Shale (right)

Fracturing in Tension, Shear or Both?

Vertical pre-cut notch ("flaw") is pressurized - Fracturing Process is observed visually and with acoustic emissions (a –Granite, b Opalinus Shale)

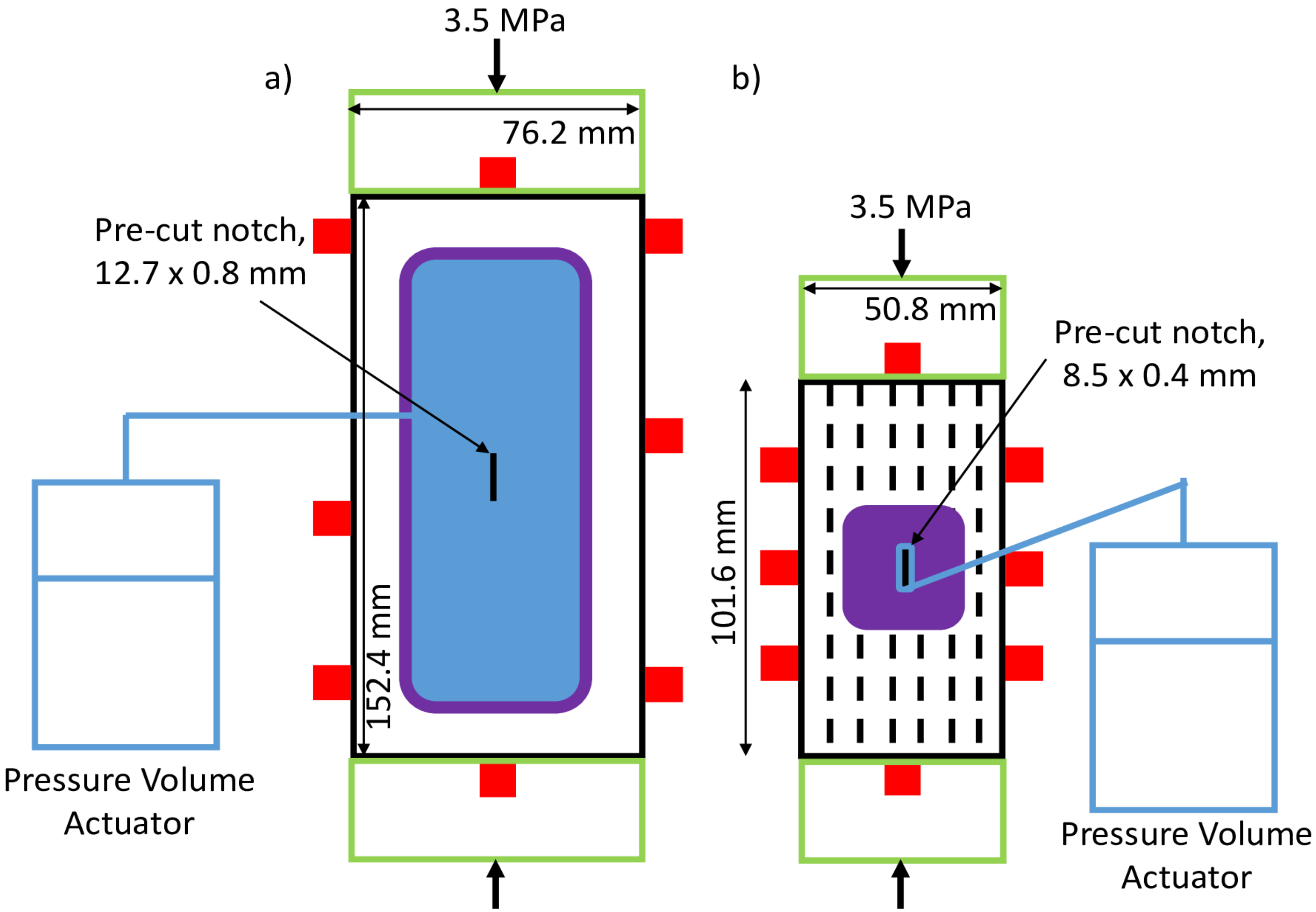

Visual Observations

Evolution of Process Zone (strains) in Granite

Top: major principal strains- Bottom: shear strains

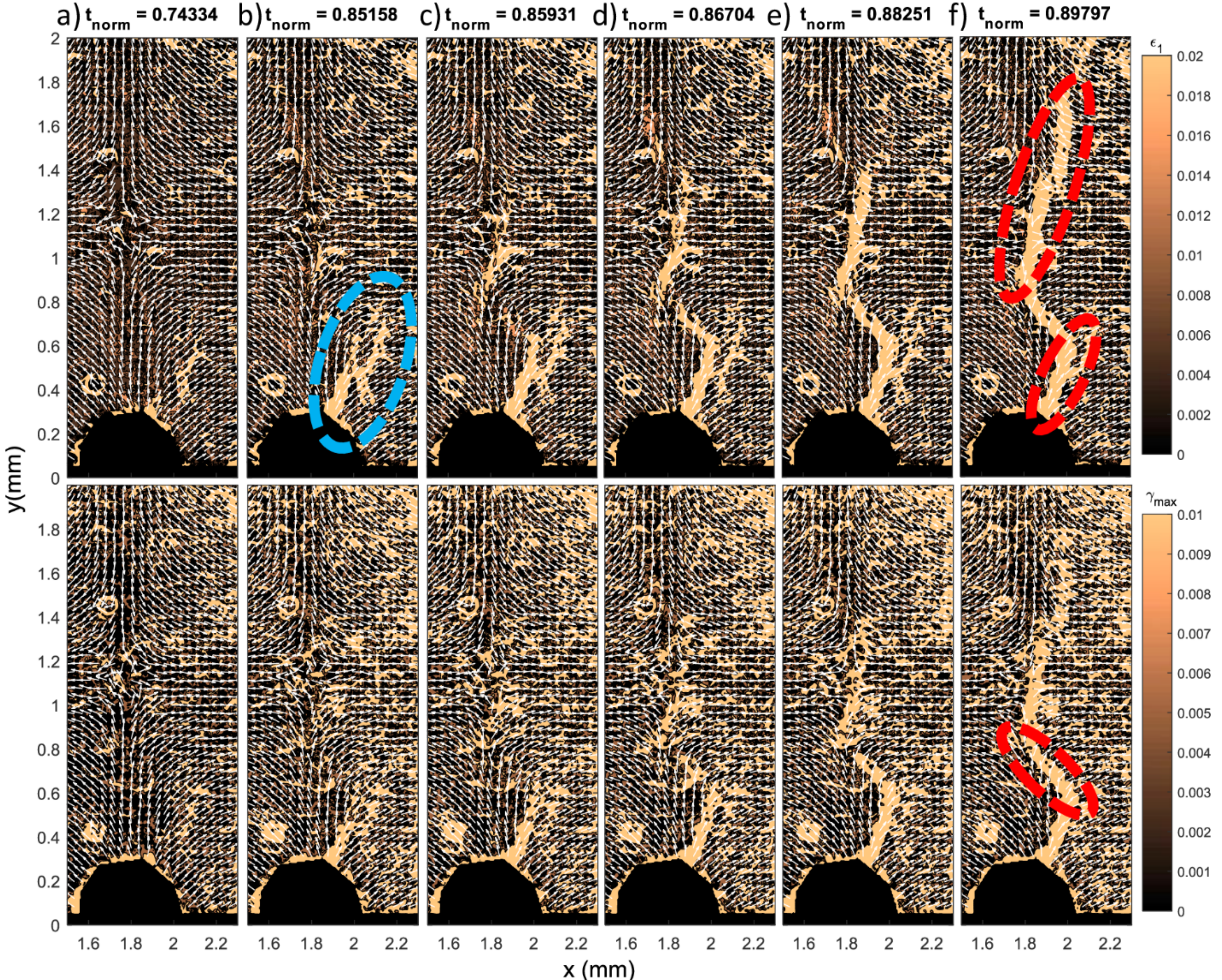

Visual Observations

Evolution of Process Zone (strains) in Shale

Top: major principal strains- Bottom: shear strains

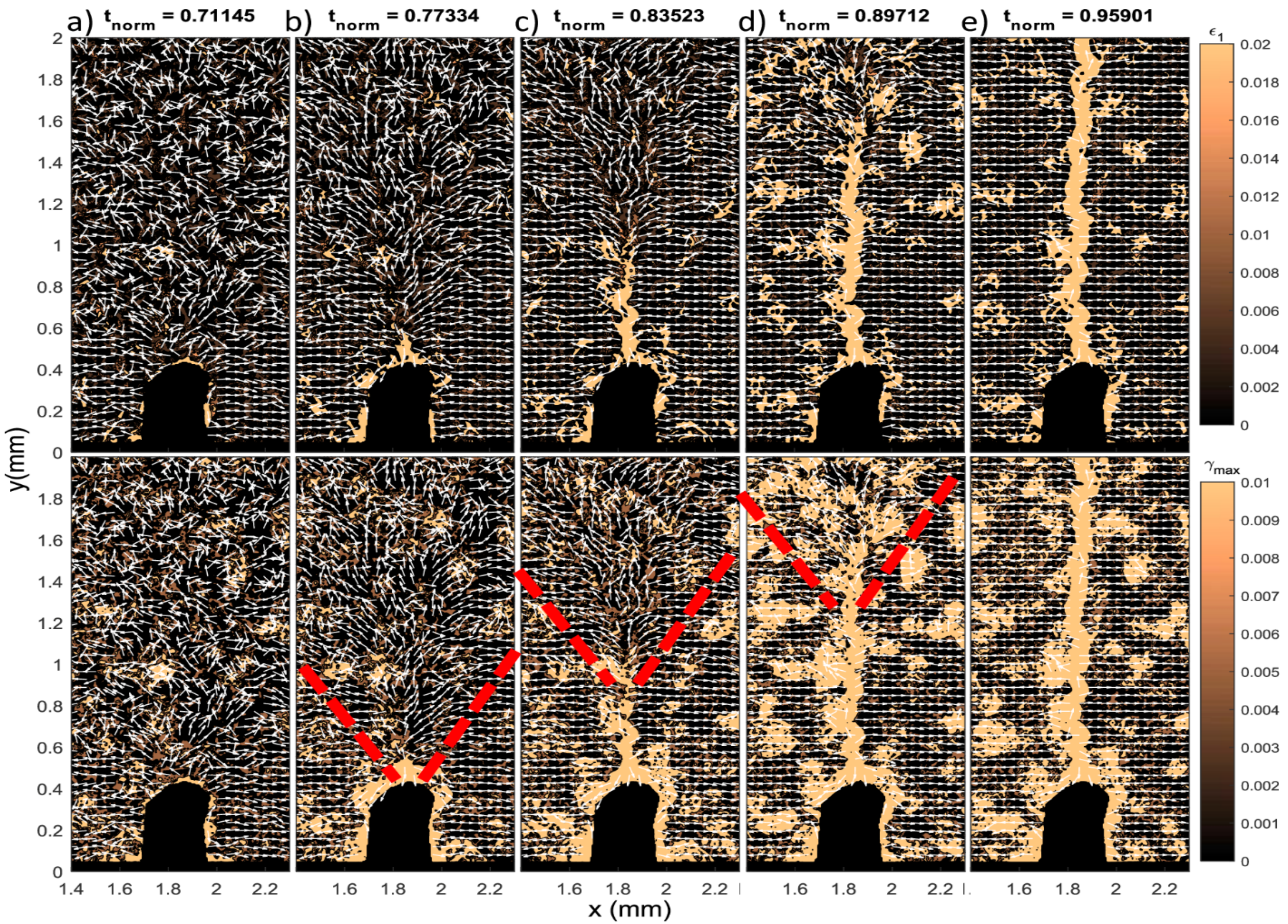

Evolution of Acoustic Emissions in Granite and Shale

Double couple (shear) and non-double couple (opening,closing) events

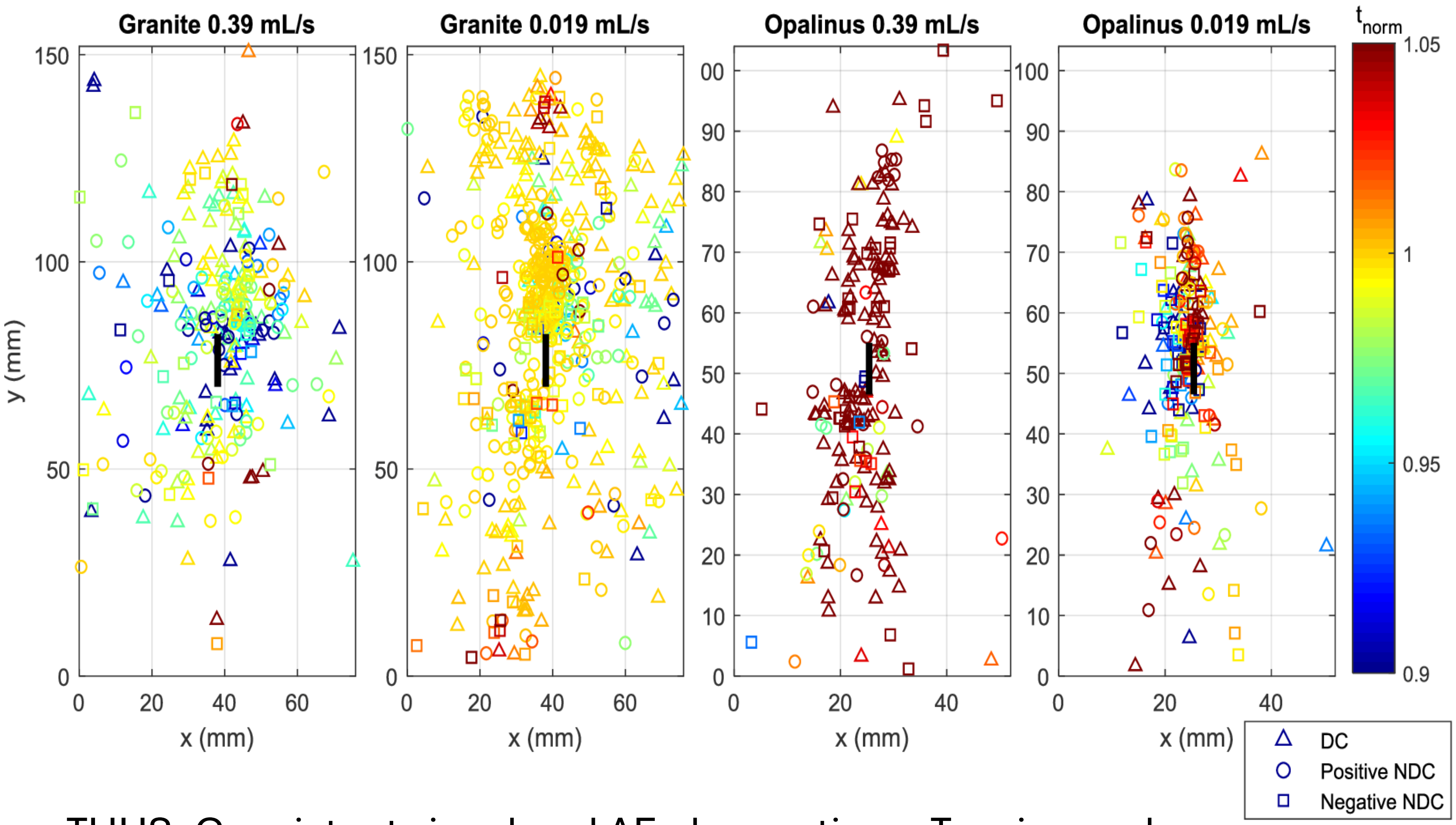

THUS: Consistent visual and AE observations: Tension and shear

Mechanics of In-situ Leaching

Background and Introduction

Discrete Fracture Network -
GEOFRAC/GEOFRAC FLOW/GEOFRAC THERMAL

Fracture Flow and Transport

Hydraulic Fracturing

Dissolution

Conclusions

Dissolution – Background on Reactive Processes

PhD Thesis Wei Li

- Reactive transport processes often induce wormholes.
- Wormholes are long, finger-like channels that form due to the flow and dissolution heterogeneity.

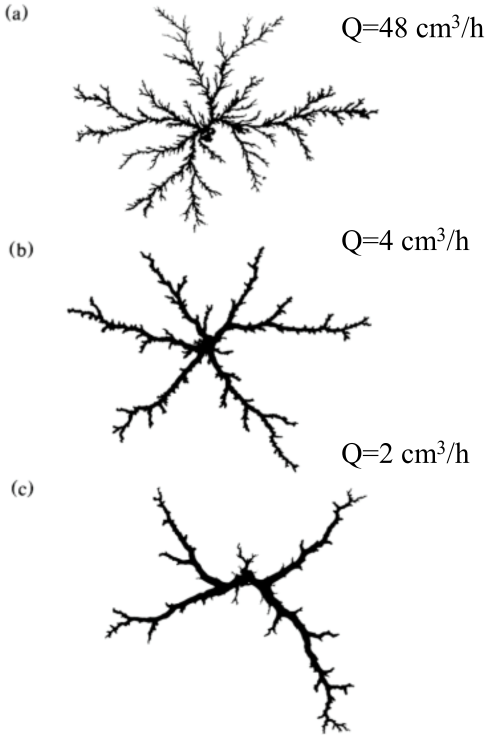

(Daccord, 1987)

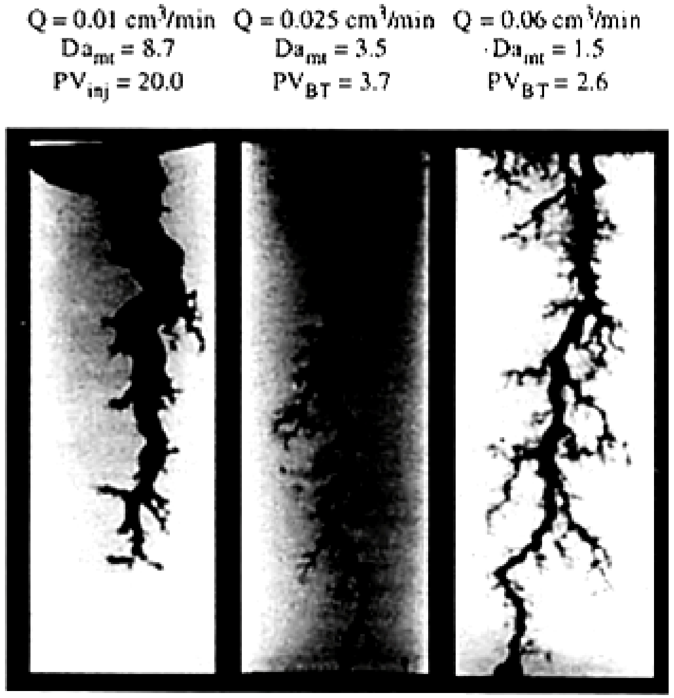

(Fredd and Fogler, 1998)

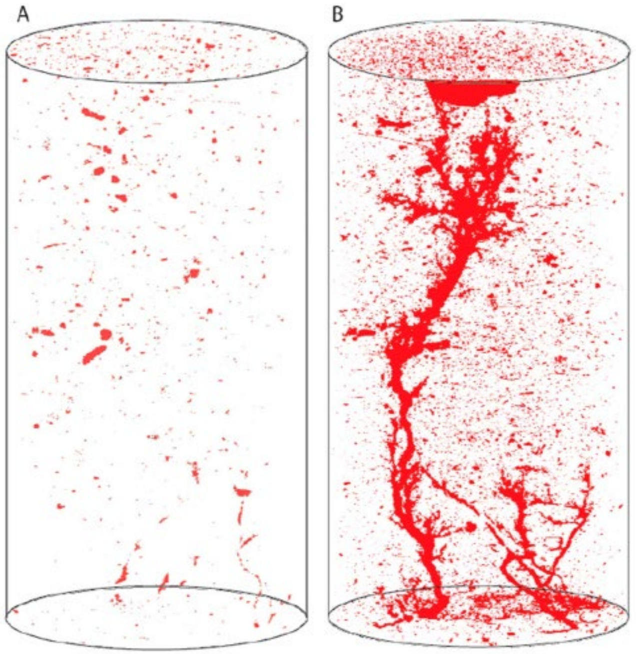

Wang et al., 2016

Evolution of dissolution kinetics during reactive transport processes

- Dissolution in an initially cylindrical tube:

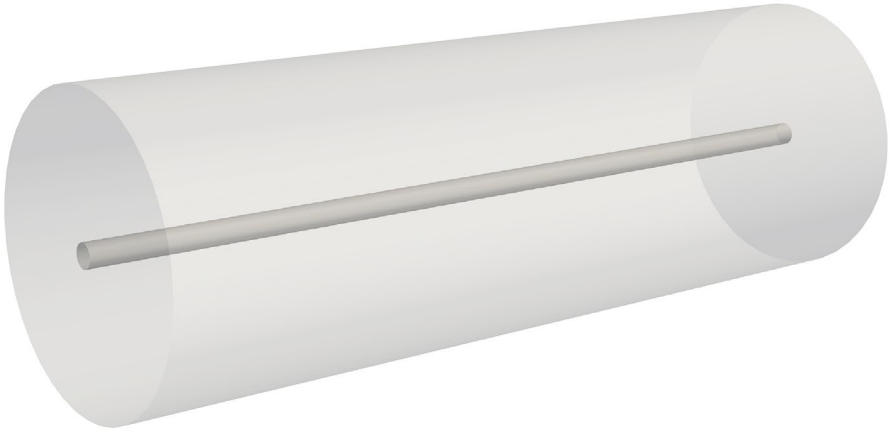

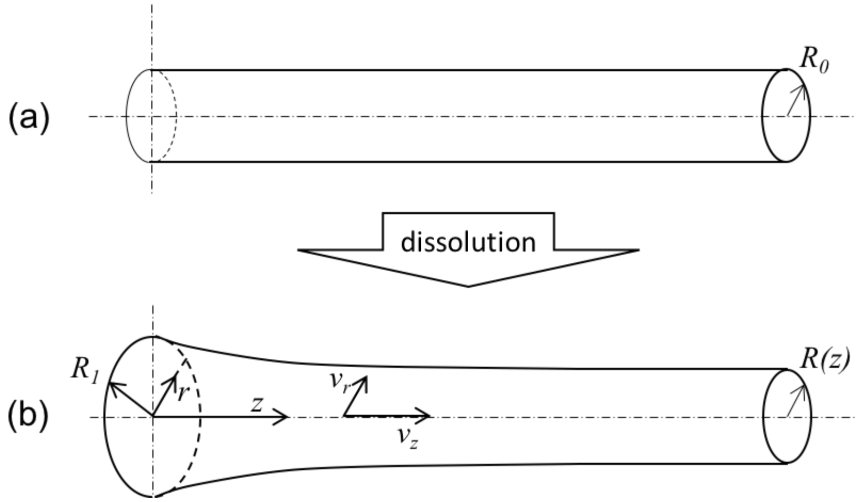

Dissolution in a Tube –Theory

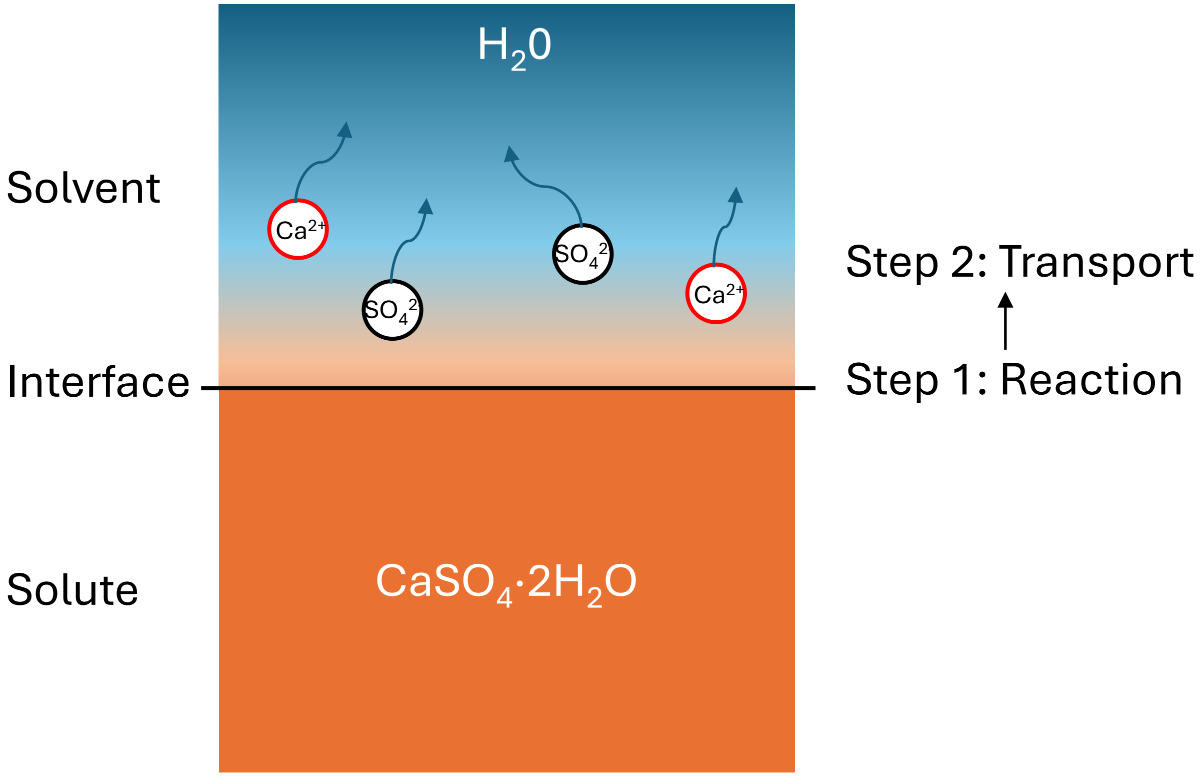

Reaction-controlled dissolution

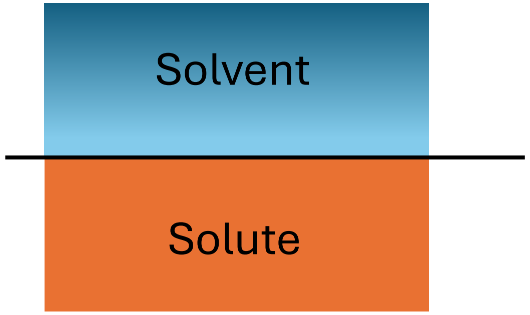

Interface is not in equilibrium
$C_i < C_{eq}$

Transport-controlled dissolution

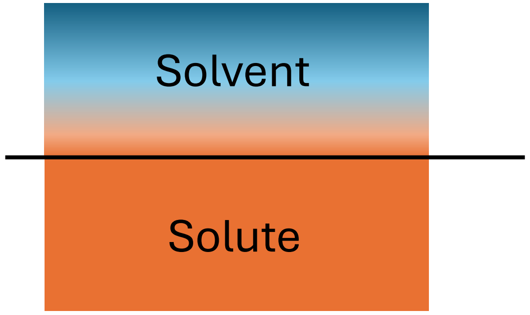

Interface is in equilibrium
$C_i = C_{eq}$

C_i : Concentration at interface
C_{eq} : Equilibrium concentration

Dissolution in a Tube –Theory

Reaction-controlled

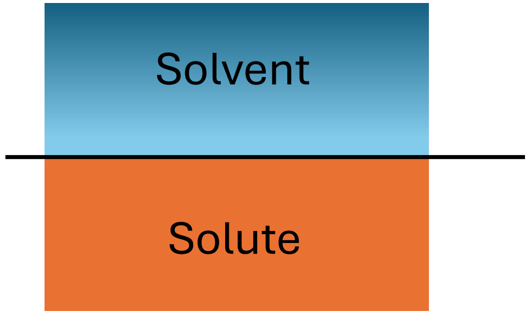

In a tube

Dissolution flux

$$q = k_r\,(C_{eq} - C_b)^n$$

k_r is the reaction rate coefficient
n is the order of reaction

Transport-controlled

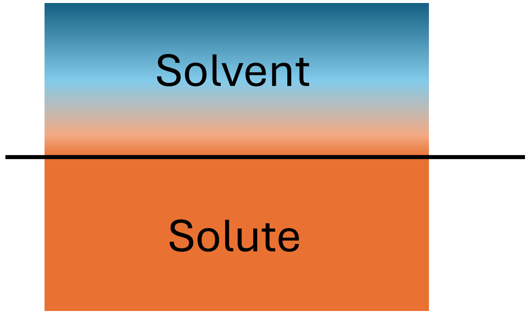

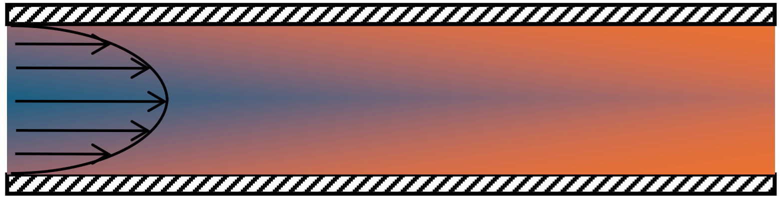

$$q = k_t\,(C_{eq} - C_b)$$

k_t is the transport rate coefficient

q is the mass flux,
C_{eq} is the equilibrium concentration,
C_b is the bulk concentration (average).

Dissolution in a Tube –Theory

- Summary
  - Extend the validity domain of the Graetz solution from a cylindrical tube to a tapered tube.
  - Sherwood number for a tapered tube is the same as that for a cylindrical tube.
  - Constant flow rate, constant effluent concentration, hence, constant overall dissolution rate, despite the enlarging of the tube.

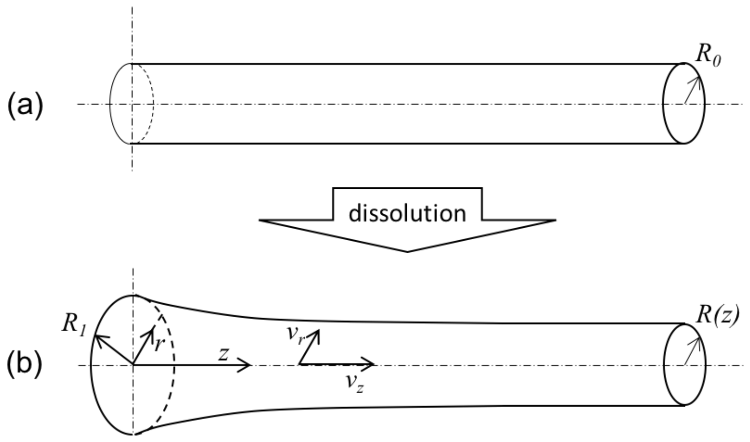

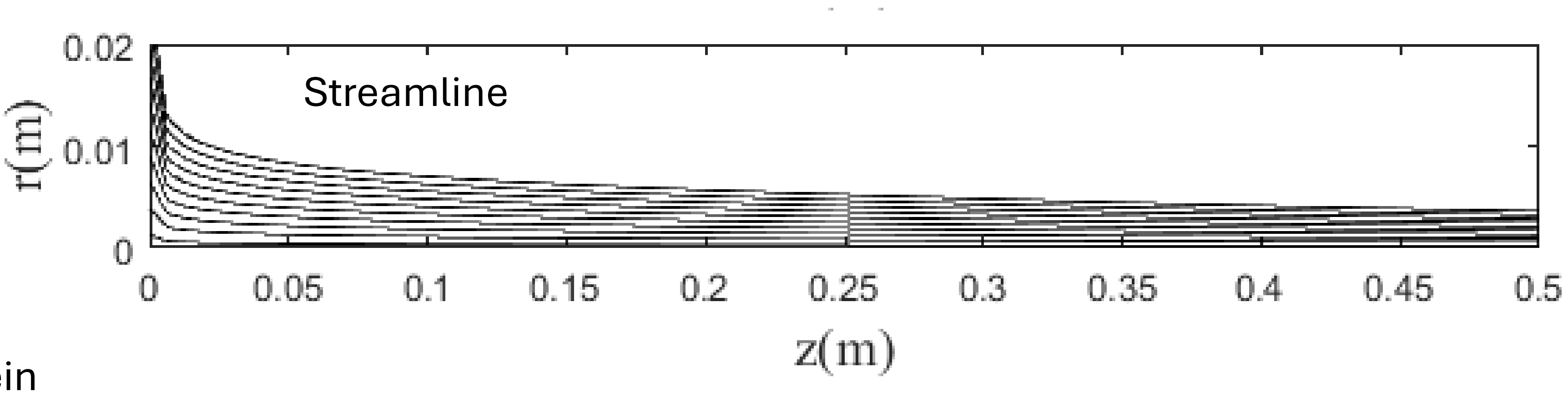

Dissolution in a Tube-Experiment

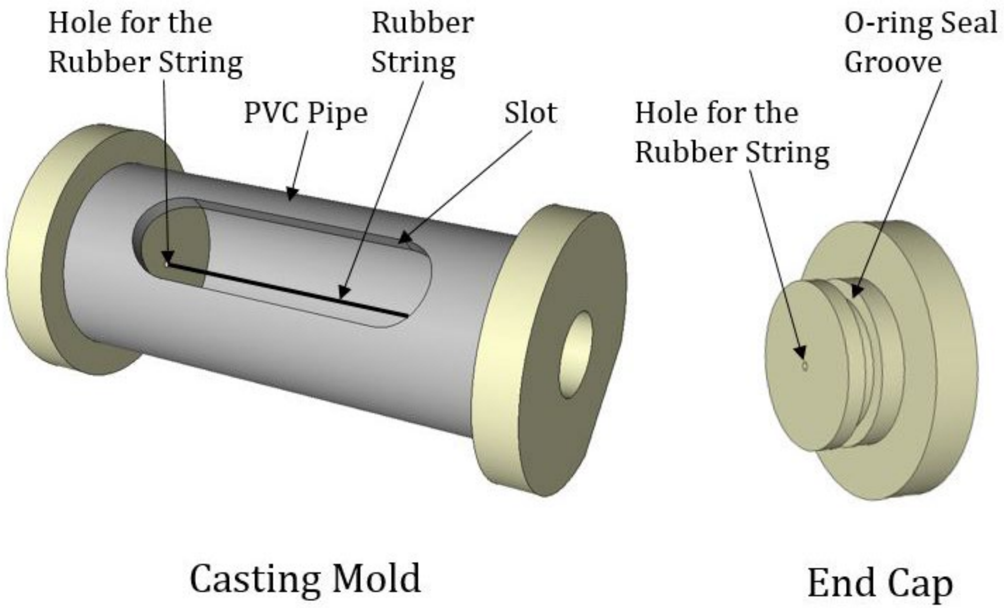

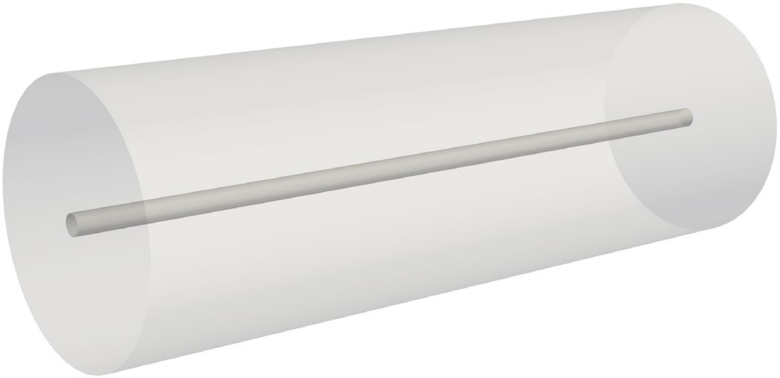

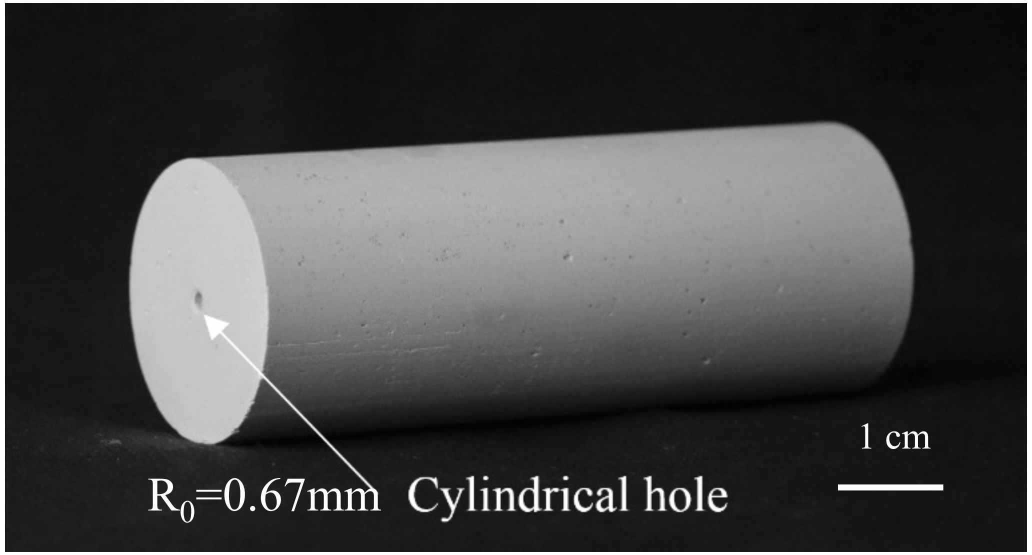

Dissolution in a Tube-Experiment

- Triaxial system
  - Control and monitor
    - Confining stress
    - Axial stress
    - Injection rate
    - Backpressure
  - Monitor
    - Inlet pressure
    - Outlet pressure
    - Axial displacement
    - Effluent concentration
    - Effluent temperature

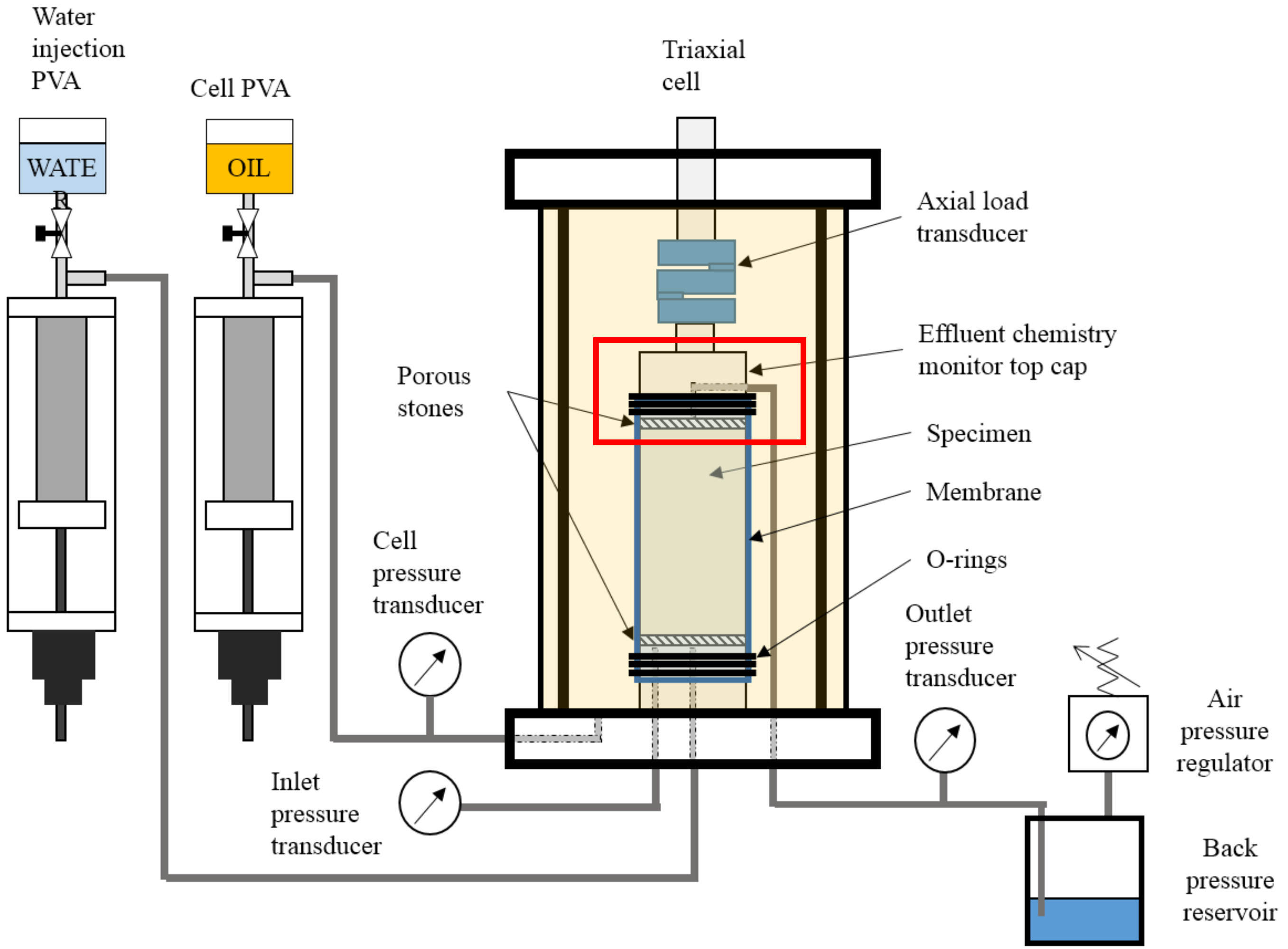

Dissolution in a Tube-Results

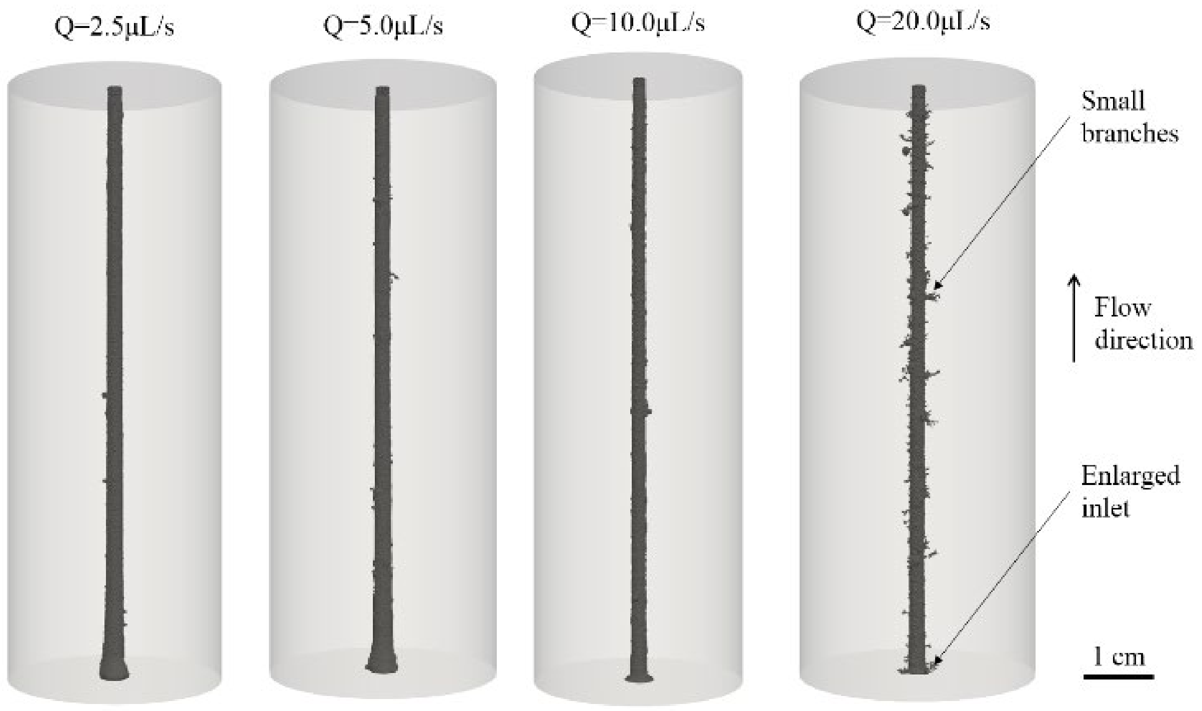

The 3D reconstructed based on the CT scan data.

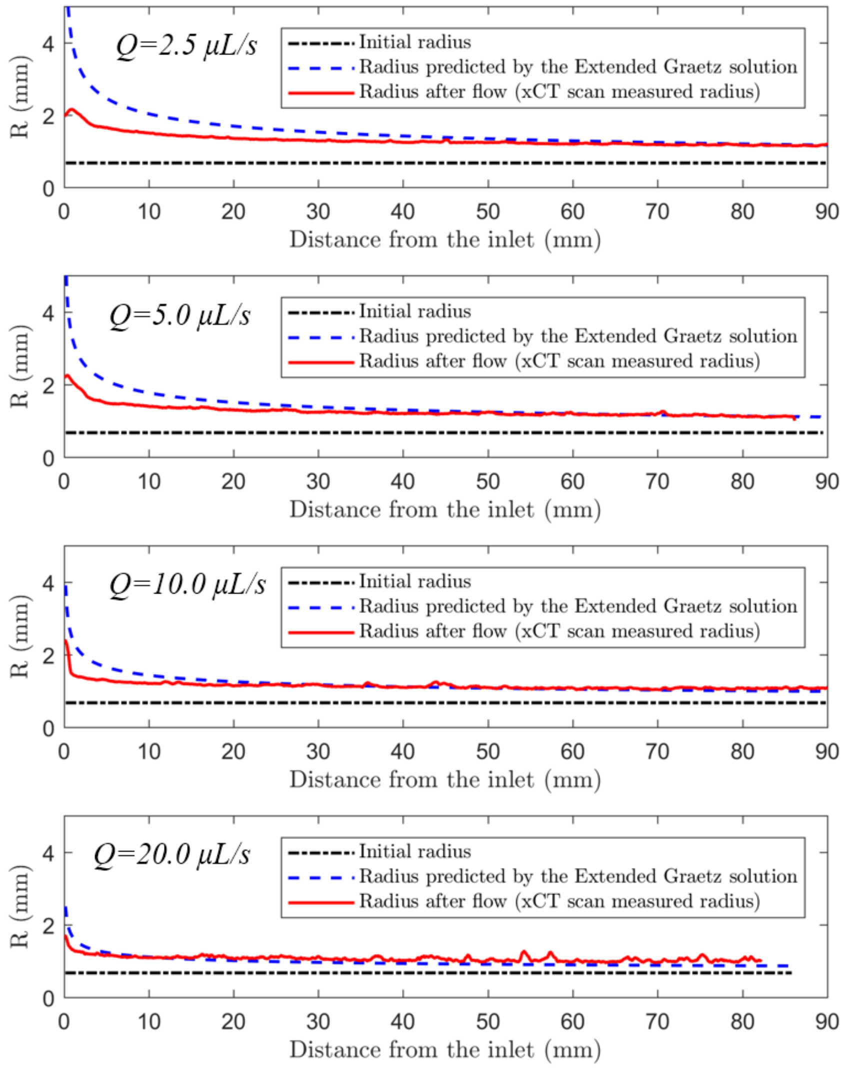

Dissolution in Porous Rock Matrix –Experiment

- Test procedure:
  - Specimen preparation

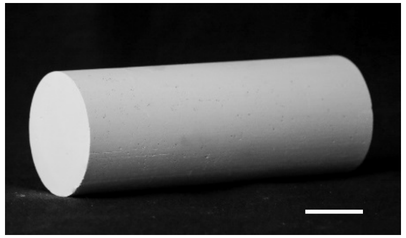

  - Test assembly

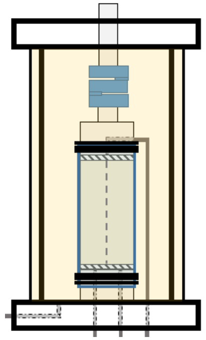

  - Overnight saturation
  - Flow 500 mL water using flow rates: 5, 7.07, 10, 14.14, 20, 28.28, 40 $\mu L/s$.
  - Dry specimen, X-ray CT sca

  - CT data analysis

Dissolution in a Porous Rock Matrix –Experiment

- Based on the effluent concentration, the core flood tests can be divided into four states:
  A. Initial transient state
  B. Mixed dissolution quasi-steady state
  C. Breakthrough transient state
  D. Wormhole dissolution quasi-steady state

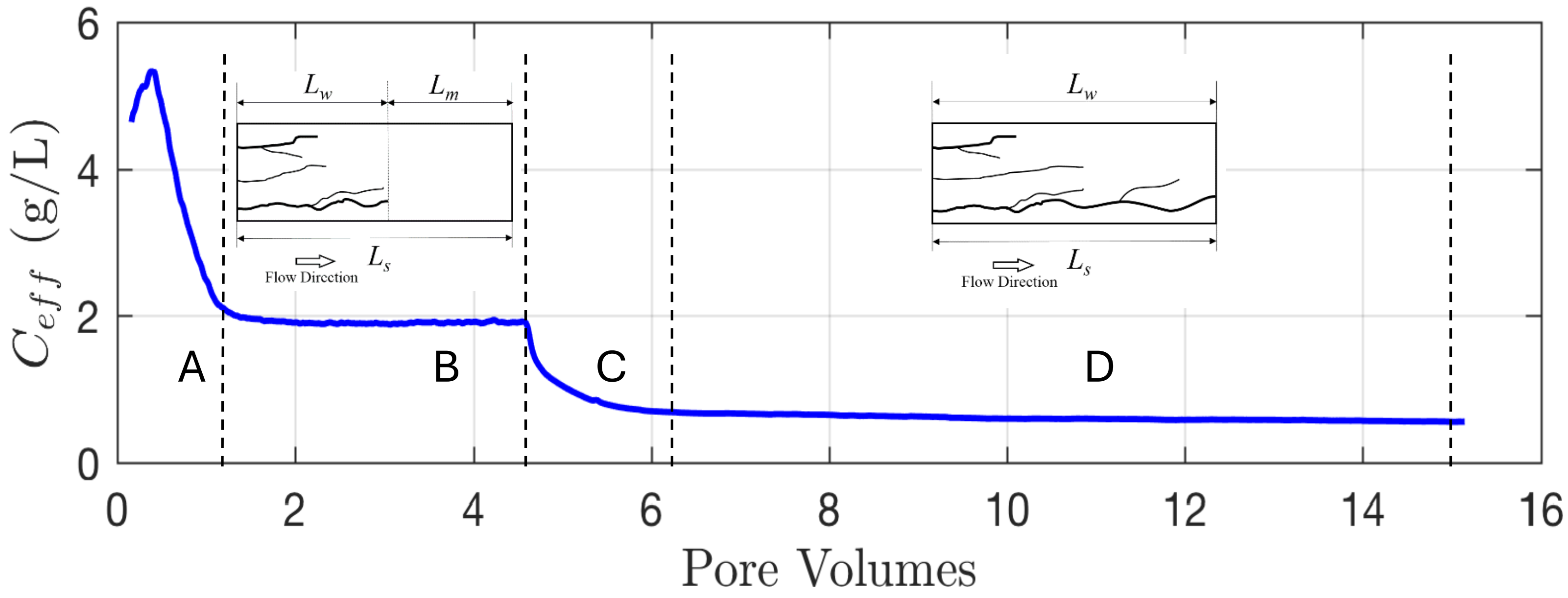

Dissolution in a Porous Rock Matrix –Theory

- Modeling the dissolution in a porous rock matrix:
  - Length of wormhole section
  - Extended Graetz solution for wormholes (tubes)
  - Continuum model for the matrix;
  - Compare constant A_e, with $A_e \sim q^{0.72}$

    A_e= Effective Surface Area

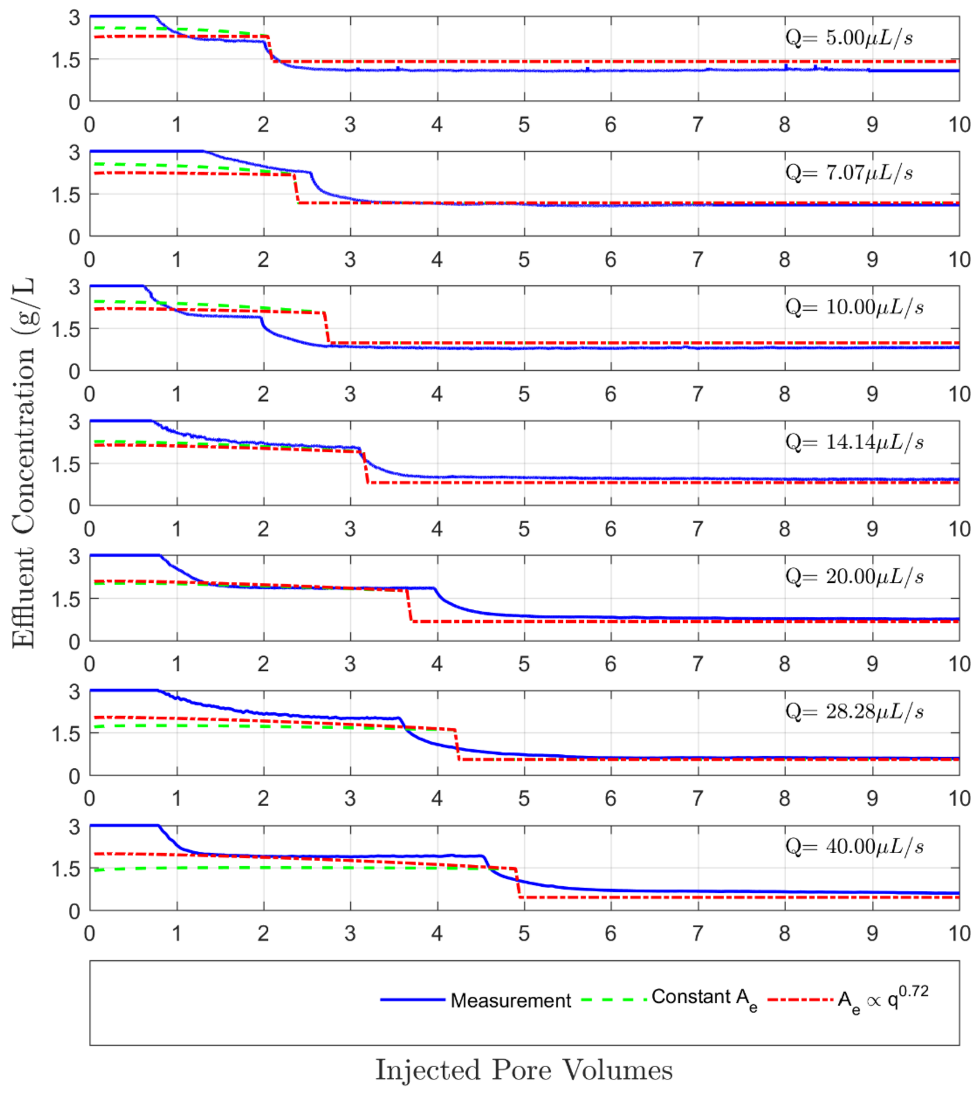

Single Fracture Experiment

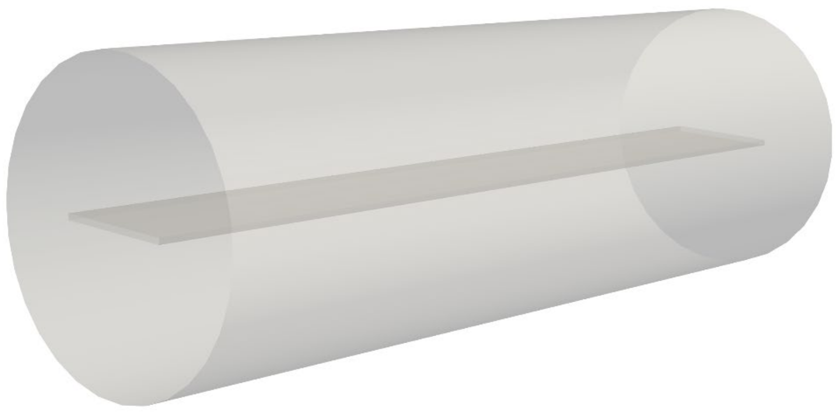

Fracture with rectangular crossection

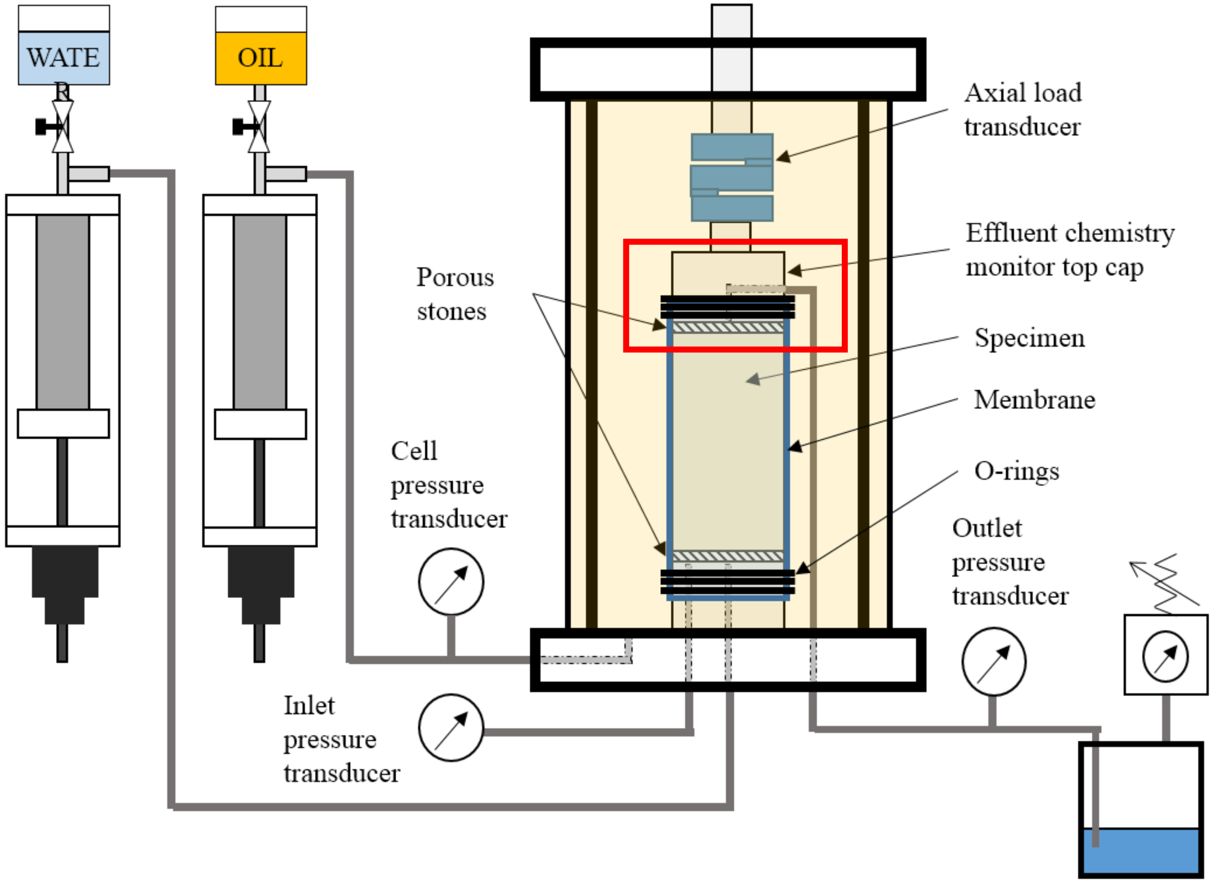

Single Fracture Experiments

Constant Geometry

1/64in=0.382mm

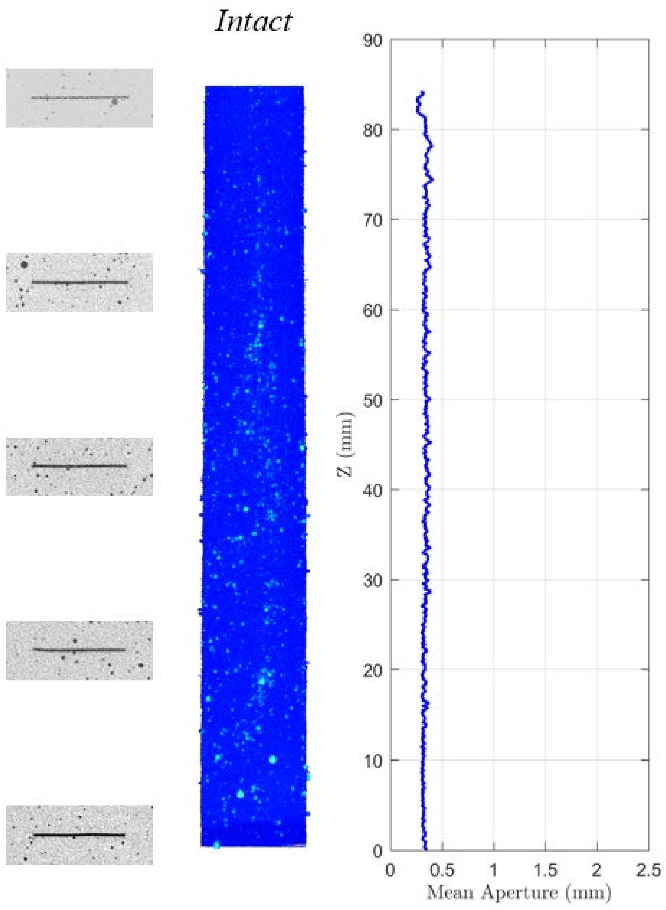

Geometry Affected by Dissolution

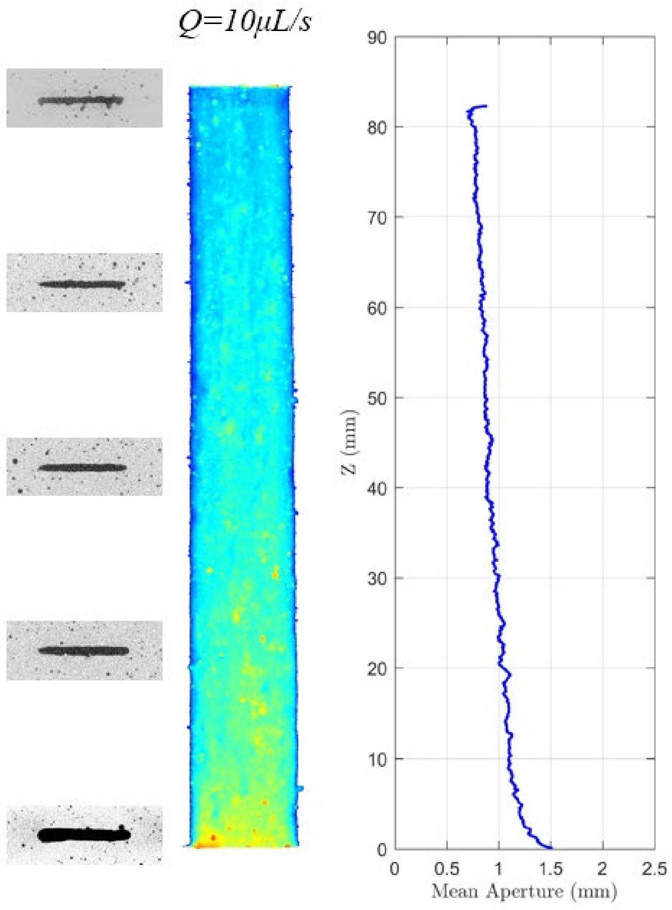

Conclusions

In-situ leaching on internal surfaces in the ground requires flow of dissolving liquid through existing openings or newly created ones and dissolution on and transport from these surfaces.

We showed that one can better understand these processes through:

DFN model GEOFRAC

Flow experiments and simulations

Hydraulic fracturing experiments

Dissolution experiments and models